HHS Public Access

Author manuscript

Cell Rep. Author manuscript; available in PMC 2023 December 05.

Published in final edited form as:

Cell Rep. 2023 October 31; 42(10): 113153. doi:10.1016/j.celrep.2023.113153.

Commensal bacteria signal through TLR5 and AhR to improve barrier integrity and prevent allergic responses to food

Andrea M. Kemter[1,6], **Robert T. Patry**[1,6], **Jack Arnold**[3], **Lauren A. Hesser**[3], **Evelyn Campbell**[5], **Edward Ionescu**[3], **Mark Mimee**[2,3,5], **Shan Wang**[1], **Cathryn R. Nagler**[1,3,4,7,*]

[1]Department of Pathology, The University of Chicago, Chicago, IL 60637, USA

[2]Department of Microbiology, The University of Chicago, Chicago, IL 60637, USA

[3]Pritzker School of Molecular Engineering, The University of Chicago, Chicago, IL 60637, USA

[4]Committee on Immunology, The University of Chicago, Chicago, IL 60637, USA

[5]Committee on Microbiology, The University of Chicago, Chicago, IL 60637, USA

[6]These authors contributed equally

[7]Lead contact

SUMMARY

The increasing prevalence of food allergies has been linked to reduced commensal microbial diversity. In this article, we describe two features of allergy-protective Clostridia that contribute to their beneficial effects. Some Clostridial taxa bear flagella (a ligand for TLR5) and produce indole (a ligand for the aryl hydrocarbon receptor [AhR]). Lysates and flagella from a Clostridia consortium induced interleukin-22 (IL-22) secretion from ileal explants. IL-22 production is abrogated in explants from mice in which TLR5 or MyD88 signaling is deficient either globally or conditionally in $CD11c^+$ antigen-presenting cells. AhR signaling in $ROR\gamma t^+$ cells is necessary for the induction of IL-22. Mice deficient in AhR in $ROR\gamma t^+$ cells exhibit increased intestinal permeability and are more susceptible to an anaphylactic response to food. Our findings implicate TLR5 and AhR signaling in a molecular mechanism by which commensal Clostridia protect against allergic responses to food.

In brief

Depletion of populations of intestinal bacteria has been associated with the increasing prevalence of food allergy. Kemter et al. show that AhR ligands and flagella from commensal Clostridia

*Correspondence: cnagler@bsd.uchicago.edu.

AUTHOR CONTRIBUTIONS

Conceptualization, A.M.K., R.T.P., and C.R.N.; methodology, A.M.K., R.T.P., J.A., M.M., and C.R.N.; analysis, A.M.K., R.T.P., J.A., and E.C.; investigation, A.M.K., R.T.P., J.A., E.C., L.A.H., E.I., and S.W.; data curation, A.M.K., R.T.P., and E.C.; writing, A.M.K., R.T.P., J.A., E.C., L.A.H., M.M., and C.R.N.; visualization, A.M.K. and R.T.P.; supervision, C.R.N.; funding acquisition, C.R.N.

SUPPLEMENTAL INFORMATION

Supplemental information can be found online at https://doi.org/10.1016/j.celrep.2023.113153.

DECLARATION OF INTERESTS

C.R.N. is a co-founder and shareholder of ClostraBio, Inc. A.M.K. is currently an employee of ALK, Hørsholm, Denmark.

regulate intestinal barrier permeability to limit allergen access to the systemic circulation and prevent allergic responses to food.

Graphical Abstract

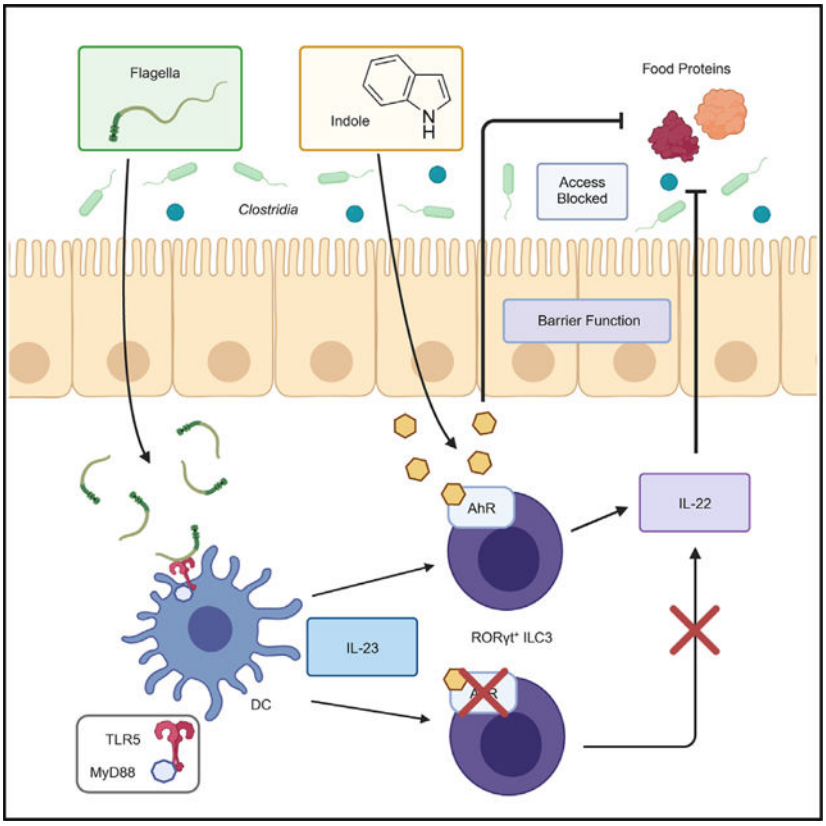

INTRODUCTION

The number of people suffering from food allergies has dramatically increased in the last 20–30 years.[1–3] It is now well accepted that 21st century lifestyle changes that reduce commensal microbial diversity are at the core of this rising prevalence.[4] The microbiota is an important driver of immune system development and education; both its composition and the timing of colonization are crucial.[5–7] We have reported a causal role for bacteria transferred from the feces of healthy, but not cow's milk allergic (CMA), infants into germ-free (GF) mice in protection against an anaphylactic response to food.[8] We defined a microbial signature that distinguished the healthy and CMA populations in both the human donors and the colonized mice. Lachnospiraceae, a family in the Clostridia class, were the dominant taxa in the healthy infant microbiota.[8] To broaden the fecal microbial signatures to a larger, more diverse group, we performed taxonomic and metabolomic analyses of samples from a cohort of twin pairs concordant and discordant for food allergy.[9] The bacteria differentially abundant between healthy and allergic twins were predominantly in the Clostridia class; the marked age range of the twins studied (6 months–70 years)

supported our premise that early-life depletion of barrier-protective Clostridia is maintained throughout life and is associated with allergic disease.[9]

These translational studies confirmed and extended earlier work, where we found that a consortium of mucosa-associated Clostridia protected mice from allergic sensitization to peanut (PN).[10] GF mice that received Clostridia-containing feces from specific-pathogen-free (SPF) mice, or from mice colonized with a consortium of spore-forming Clostridia, were protected against allergic sensitization to food. The observed reduction in intestinal barrier permeability was dependent on Clostridia-induced interleukin-22 (IL-22) production. IL-22 is a member of the IL-10 cytokine family with known barrier-protective functions including stimulation of repair mechanisms and epithelial cell proliferation,[11–13] glycosylation,[14,15] mucus production,[16] and induction of antimicrobial peptides (AMPs) such as Reg3β and Reg3γ.[17,18] In the intestinal tract, IL-22 is mainly produced by type 3 innate lymphoid cells (ILC3s) in response to bacterial metabolites such aryl hydrocarbon receptor (AhR) ligands[19] and short-chain fatty acids (SCFAs)[20] or IL-23 produced by antigen-presenting cells (APCs) that recognize bacterial structures,[21–24] including flagellin.[25] Flagellin is the ligand for TLR5[26] and the primary component of flagella, protein filaments used for bacterial motility.[27] Some Clostridia possess functional flagella, which activate TLR5 to varying degrees.[28–30] Clostridia also produce SCFAs and AhR ligands. We have recently shown that delivery of butyrate to the lower gastrointestinal tract (using a novel polymeric micelle) is sufficient to prevent an allergic response to food in a therapeutic model.[31] We have also reported that monocolonization with a butyrate-producing Clostridial strain, *A. caccae*, mimicked the effects of the healthy microbiota and prevented an anaphylactic response to a food allergen.[8] *A. caccae* is non-motile and does not produce indoles (major AhR ligands). Butyrate production therefore seems to comprise one bacteria-induced barrier-protective pathway.

In this article, we examine whether the interaction of bacterial flagella and indoles with their host receptors comprises a second bacteria-induced barrier-protective pathway induced by a consortium of Clostridia. We identified taxa in the consortium that possess flagella and produce indole. Lysates and flagella isolated from this Clostridia consortium induced IL-22 secretion from ileal explants. IL-22 production was not detectable in explants from mice with a deficiency in TLR5 or MyD88 signaling either globally or conditionally in $CD11c^+$ cells. Treatment of mice with flagella prepared from the Clostridia consortium (Fla-C), but not flagellin from a pathogen (Fla-ST [flagellin from *Salmonella enterica* serovar Typhimurium]), led to a significant reduction in intestinal barrier permeability in antibiotic (Abx)-treated mice. AhR signaling in $ROR\gamma t^+$ cells was necessary for IL-22 induction by both Fla-ST and Fla-C. Daily gavage of indole to Abx-treated weanling mice reduced intestinal permeability in an IL-22-independent manner. Mice deficient in AhR in $ROR\gamma t^+$ cells exhibited an increase in intestinal permeability to fluorescein isothiocyanate (FITC)-dextran and were more susceptible to an anaphylactic response to food. Taken together, our results define a molecular mechanism by which two microbial products (commensal Clostridial flagella signaling through TLR5 and indole signaling through the AhR) act synergistically on cells of the immune system to elicit a response that protects against food allergy.

RESULTS

Taxa in the Clostridia consortium are flagellated and produce indole and butyrate

To examine the components that influence IL-22 production in a murine Clostridia consortium, we first generated a mixed *in vitro* culture of these organisms for more in-depth analyses. Shotgun metagenomic sequencing of this cultured consortium confirmed that their taxonomic composition was largely similar to a previously reported Clostridia consortium,[10] with *Lachnospiraceae* being particularly abundant (Figure 1A). Functional genomic analysis of the metagenomic data revealed the relative abundance of species that contain protein domains for genes involved in the production of flagellin (21.2%), indole as a representative AhR ligand (22.4%), and butyrate (8.9%) and estimated the number of taxa in this consortium that could produce these bacterial molecules and metabolites (Figure 1B). Next, we performed *in vitro* assays to examine the ability of the cultured consortium to make these products. Evidence of migration in motility agar confirmed that the consortium contained motile bacteria likely possessing flagella (Figure 1C). Analysis of culture supernatants by high-performance liquid chromatography (HPLC) UV-visible (UV-vis) demonstrated production of butyrate (Figure 1D). Application of Kovac's reagent, which turns red upon exposure to indole, indicated the presence of indole in Clostridia consortium cultures (Figure 1E). Additionally, indole as well as related indole-containing compounds were detectable in feces of mice colonized with spores prepared from the Clostridia consortium cultures, or by transfer of feces from these mice as donors, when compared with GF mice (Figure 1F). We were able to culture two isolates from the consortium most closely related to the *Lachnospiraceae* (represented using a phylogenetic tree in Figure S1A). They were both motile (Figure S1B) and bore flagella that signal through TLR5 (Figure S1C). In addition, we cultured each of these organisms in a mixture with an indole producer most closely related to the *Oscillospiraceae*, which was dependent on the *Lachnospiraceae* to grow *in vitro* (Figure S1A). These mixtures (LachOS_1 and LachOS_2) both produce indole (Figure S1D), but only LachOS_1 produced butyrate (Figure S1E). With evidence for the presence of flagellated as well as indole-producing bacteria in the Clostridia consortium, we characterized the potential impact of these microbial products on allergic sensitization.

Clostridia lysates induce intestinal IL-22 through TLR5 and MyD88

After determining that the Clostridia consortium contained flagellated taxa, we examined whether the consortium contained a TLR5 ligand that induced intestinal IL-22 production. First, we generated lysates from consortium cultures (see STAR Methods) to use as a crude, flagella-containing preparation for *in vitro* analysis. Stimulation of ileal lamina propria (LP) tissue (ileal tissue with intestinal epithelial cells [IECs] removed[25,32]) from Abx-treated C57BL/6 mice with Clostridial lysates for 45 (Figure 2A) or 90 min (Figure S2A) induced expression of both IL-23 subunits (IL-23A and IL-12B) to an extent comparable to purified Fla-ST. The Clostridial lysates induced production of IL-22 from whole ileum (Figure 2B) and colon (Figure S2B) explants from Abx-treated C57BL/6 mice at a level comparable to Fla-ST. Since flagellin signals through TLR5 and MyD88 to induce downstream IL-22 production,[26] we incubated ileal explants from Abx-treated mice deficient in either TLR5 or MyD88 with Clostridial lysates or Fla-ST. As expected, ileal explants from *Tlr5*$^{-/-}$ or *Myd88*$^{-/-}$ mice produced little or no IL-22 after stimulation with Clostridial lysates or

Fla-ST, unlike explants from their heterozygous *Tlr5*$^{+/-}$ or *Myd88*$^{+/-}$ littermates or from either group stimulated with IL-23 (Figures 2C and 2D). To examine whether CD11c^{+} intestinal APCs were the primary cells recognizing the TLR5 ligand in Clostridial lysates, we stimulated ileal explants from Abx-treated *Cd11c*^{Cre} *Myd88* $^{fl/fl}$ or *Cd11c*^{Cre} *Tlr5*$^{fl/fl}$ mice, which lack TLR5 or MyD88 signaling specifically in CD11c^{+} APCs. Explants from Cre^{+} mice were unable to produce IL-22, unlike those from their Cre^{-} littermates (Figures 2E and 2F), confirming the crucial role of CD11c^{+} APCs in recognizing flagellin. These results show that lysates from bacteria in the Clostridia consortium contain flagella that can be recognized by intestinal CD11c^{+} APCs and that signal through TLR5 and MyD88 to induce IL-22 production.

Commensal Clostridia flagella induce intestinal IL-22 and reduce barrier permeability *in vivo*

To examine the effect of treatment with commensal Clostridia flagella *in vivo*, we pooled preparations from Clostridia consortium cultures enriched for flagella (Figure S3A) and confirmed that the product signaled through TLR5 when compared to Fla-ST at equivalent total protein concentrations (determined by BCA assay) (Figure S3B). The product (Fla-C) also induced IL-22 in ileal explant cultures in a dose-dependent manner and comparably to Fla-ST at the same protein concentration (Figure 3A). IL-22 induction by Fla-C was dependent on TLR5 (Figure 3B) and independent of TLR4 signaling (Figure S3C). Finally, we examined whether this flagellar preparation modulated intestinal barrier permeability. After neonatal Abx treatment, we intraperitoneally (i.p.) injected mice with Fla-C on days 1, 3, and 5 post-weaning and examined intestinal permeability to FITC-dextran on day 6. The concentration of FITC-dextran was significantly reduced in the serum of Fla-C-treated mice compared with PBS-treated littermates (Figures 3C and S3D). Interestingly, unlike Fla-C, Fla-ST did not reduce permeability to FITC-dextran. Mice injected with 5 μg Fla-C had significantly reduced serum FITC-dextran concentrations when compared with littermates injected with the same amount of Fla-ST or PBS (Figure 3C). This was not due to an inability of Fla-ST to induce IL-22 *in vivo*. A single i.p. injection of Fla-ST at weaning was sufficient to increase IL-22 production from both ileum and colon explants in a dose-dependent manner (Figures S3E and S3F). Earlier work showed that repeated i.p. injections of Abx-treated adult mice with Fla-ST induced elevated expression of the AMPs Reg3β and -γ in whole ileal tissue.[32] When we examined AMP expression in whole colon and ileal tissues from the neonatal Abx-treated mice in Figure 3C by qRT-PCR, we found that Fla-ST induced the expression of Reg3β and -γ to a significantly greater extent than Fla-C (Figures 3D and 3E). Both Fla-C and Fla-ST treatments significantly reduced expression of the proinflammatory cytokines interferon γ (IFN-γ) (Figure S3G) and tumor necrosis factor α (TNF-α) (Figure S3H), as well as the anti-inflammatory cytokine IL-10 (Figure S3I), in the ileum compared to PBS controls. IL-17A expression was induced by Fla-ST, but not Fla-C, in the colon (Figure 3F) and to a lesser extent in the ileum (Figure S3J). Increased serum concentrations of the proinflammatory cytokine IL-6 and the neutrophil-attracting chemokine CXCL1 have also been reported after i.p. injection of Fla-ST in adult mice.[30,33] When we examined serum from mice 2 h after i.p. injection with each flagellar preparation, we found that Fla-ST induced significantly higher levels of serum IL-6 and CXCL1 than Fla-C (Figures 3G and 3H). Other work has shown that flagella from different bacteria

can have disparate effects on the host immune system due to changes in their amino acid sequence.[34] Since we had isolated and sequenced the genomes of Lach_1 and Lach_2, two representative flagella-producing taxa in the Clostridia consortium, we examined the amino acid sequences of their predicted flagellin proteins to determine if they differ substantially from *Salmonella* FliC. After examination of the predicted protein structure (Figure S4A) and alignment of their amino acid sequences (Figure S4B), the Clostridia flagellins were more like one another (particularly at the N and C termini) than *Salmonella* FliC. This included differences in several amino acids known to be key for TLR5 binding in the D1 domain (denoted by black asterisks in Figure S4B).[35] The *Salmonella* FliC was also accompanied by a very distinct flagellar operon, while those from Lach_1 and Lach_2 were more similar (Figure S4C). These experiments show that flagella enriched from the Clostridia consortium induce IL-22 in a TLR5-dependent manner. Clostridial flagella also reduced epithelial permeability to FITC-dextran.

Indole has a barrier-protective effect independent of its induction of IL-22

In addition to the presence of flagellated bacteria in the Clostridia consortium cultures, we also detected production of the AhR ligand indole (Figures 1E, 1F, and S1D). Since AhR-deficient mice are impaired in their production of IL-22,[36] we hypothesized that the production of AhR ligands by commensal Clostridia contribute to the barrier-protective response that they induce. We therefore tested whether indole induced IL-22 production in ileal explants from Abx-treated mice. IL-22 production was significantly induced in response to 10 ng/mL indole but to a much lower extent than stimulation with IL-23 (Figure 4A). We also examined indole's ability to induce IL-22 at the transcript level in LP tissues, where half of each ileum was left untreated while the other half was stimulated with indole (Figure 4B). Induction of IL-22 was dependent on AhR signaling in RORγt$^+$ cells (Figure 4C), which include ILC3s and T cells.[37,38] Neonatal Abx-treated mice that received daily intragastric (i.g.) gavage of indole also had reduced concentrations of FITC-dextran measurable in their serum compared with their water-gavaged littermates (Figure 4D). However, daily treatment with indole did not result in elevated expression of the IL-22 target gene *Reg3b* (Figure 4E). Co-administration of a neutralizing antibody to IL-22 reduced *Reg3b* expression but did not impair the indole-induced reduction in intestinal barrier permeability (Figure 4F). These results suggest that while indole acts as an AhR ligand to induce IL-22 production, it may also have an IL-22-in-dependent barrier-protective effect.

AhR signaling in RORγt$^+$ cells is necessary for IL-22 induction and protection against allergic responses to food

We previously reported that most of the IL-22 induced by colonization of GF mice with a consortium of Clostridia was produced by CD3$^-$RORγt$^+$ ILC3s.[10] We also detected some production of IL-22 from CD4$^+$TCRβ^+ T cells.[10] We showed that Clostridia induced IL-22-regulated intestinal permeability to a food antigen and prevented allergic sensitization to food.[10] AhR signaling has a central role in the maintenance of mucosal homeostasis.[39] Importantly, AhR signaling is critical to the maintenance of ILC3s and their functional capacity to produce IL-22.[36] In this article, we show that Clostridial lysates or flagellar preparations induce IL-22 production by activating CD11c$^+$ APCs in a TLR5-dependent

manner (Figure 2). To examine whether AhR signaling by RORγt$^+$ ILC3s regulates this process, we stimulated ileal explants from Abx-treated *Rorgt^{Cre} Ahr$^{fl/fl}$* mice with both Fla-ST and Fla-C (Figures 5A and 5B). IL-22 was secreted in response to stimulation with IL-23 but not Fla-ST (Figure 5A) or Fla-C (Figure 5B), indicating that, in the absence of AhR signaling, ILC3s can respond to direct stimulation with IL-23 but not to TLR5-dependent stimuli. Ileum (Figure 5C) and colon (Figure S5A) explants from untreated *Rorgt^{Cre}Ahr$^{fl/fl}$* mice produced significantly lower levels of IL-22 than explants from their wild-type (WT) Cre$^-$ littermates, suggesting defective production of IL-22 at baseline.

Intestinal permeability to FITC-dextran was significantly increased in mice that lacked functional AhR signaling in RORγt$^+$ ILC3s (Figure 5D). To examine whether this deficiency also altered intestinal permeability to food antigens, we sensitized and challenged *Rorgt^{Cre}Ahr$^{fl/fl}$* mice according to the schematic in Figure 5E. Increased PN-specific type 2 responses were already apparent on day 17 post-weaning (after three sensitization doses), as splenocytes from Cre$^+$ mice restimulated with PN protein produced significantly higher levels of IL-13 than their Cre$^-$ littermates (Figure 5F). *Rorgt^{Cre}Ahr$^{fl/fl}$* mice that underwent the full sensitization protocol were more susceptible to an anaphylactic response to food, demonstrated by an increase in PN-specific serum immunoglobulin E (IgE) and IgG1 (Figure 5G) and significantly higher reductions in core body temperature at challenge (Figure 5H). We did not observe significant changes in the percentages or numbers of RORγt$^+$ ILC3s or T cells associated with each genotype (Figures S5B–S5E). These results show that AhR signaling in RORγt$^+$ cells is required for Clostridia-induced protection against an allergic response to food.

DISCUSSION

We have previously reported that a bacteria-induced barrier-protective response is required to prevent allergic sensitization to food in mice.[10] IL-22 production by ILC3s was a crucial mediator of the Clostridia-induced barrier-protective response in mice. Alteration of commensal bacterial community structure by neonatal Abx treatment resulted in increased permeability to PN allergens and their detection in serum after oral PN gavage. Administration of a consortium of Clostridia or an IL-22 fusion protein to Abx-treated mice significantly reduced serum concentrations of PN allergens.[10] When mice that received the Clostridia consortium were treated with a neutralizing antibody to anti-IL-22, the detection of PN allergens in serum was significantly elevated, demonstrating that Clostridia-induced IL-22 was necessary and sufficient to regulate allergen access to the systemic circulation. We have shown that butyrate-producing Clostridia[8] and administration of a polymeric butyrate-containing micelle[31] are effective in preventing and treating an allergic response to food. In this article, we have characterized butyrate-independent pathways by which taxa in the Clostridia consortium that are flagellated and produce indoles modulate epithelial barrier permeability.

Bacterial flagellin induces the expression of IL-23 in dendritic cells of the small intestinal LP by signaling through TLR5, which then stimulates IL-22 production primarily by RORγt$^+$ ILC3s.[25] Using mice deficient in TLR5 and MyD88 signaling both globally and conditionally in CD11c$^+$ cells, we showed that Clostridial lysates require this pathway

to induce IL-22, suggesting that flagella are an important mediator of Clostridia-host interactions. Comparison of *S. Typhimurium* flagellin with flagella enriched from the Clostridia consortium showed that both induce IL-22 production by ileal explants to a similar level. However, Fla-C was able to reduce intestinal permeability to FITC-dextran, where Fla-ST did not. This differential impact on permeability was accompanied by discordant stimulation of some key host immune effectors. While treatment with either Fla-C or Fla-ST reduced expression of IFN-γ, TNF-α, and IL-10, the induction of Reg3 AMPs was significantly greater for Fla-ST than Fla-C. This suggests that while the induction of IL-22 from Fla-ST and Fla-C was comparable *ex vivo*, the downstream impacts *in vivo* were quite different. Indeed, the influence of IL-22 on the intestinal mucosa is context dependent.[40] In some settings, IL-22 can promote intestinal inflammation.[41,42] Treatment with Fla-ST induced elevated levels of the neutrophil-attracting chemokine CXCL1 and proinflammatory cytokine IL-6 when compared with Fla-C. We showed that there are differences in the amino acid sequences of selected flagellins from two isolates of the consortium from which Fla-C was enriched when compared with Fla-ST, particularly in the domains making up the hypervariable region.[43] Changes to the amino acid sequence of flagellin can have significant impacts on its signaling. In addition, we showed that the flagellar operons of *S. Typhimurium* and the two Clostridial isolates are quite distinct. TLR5 signaling also induces non-IL-22-mediated responses in epithelial cells, which might contribute to barrier permeability and downstream host responses.[44] Our data suggest that flagella from non-invasive, mucosa-associated commensals gain access to the intestinal LP to modulate intestinal permeability. The homeostatic response to commensal flagella may be distinct from that induced in the context of pathogenic inflammation. In the small intestine, where food is normally absorbed, epithelial TLR5 expression is restricted to Paneth cells.[44] Differential signaling via TLR5 may also trigger the release of Paneth cell AMPs in a context-dependent fashion with concomitant effects on intestinal permeability.[44]

Multiple studies have demonstrated that the AhR plays a crucial role in maintaining the barrier function of the intestinal epithelium.[36,39,45–47] We show here that commensal Clostridia produce indole-containing compounds and that indole induces IL-22 while reducing intestinal permeability. The impact of indole on intestinal barrier function seemed to be independent of IL-22 induction, suggesting an additional mechanism for the barrier-protective effect of indole that must be explored in future studies. Numerous cell types, including IECs as well as neurons, express AhR,[39] and IL-22-independent effects could potentially be triggered by indole gavage. AhR signaling may also have effects independent of the induction of a gut barrier-protective response. Earlier work showed that colonization of GF mice with a consortium of Clostridia significantly increased the production of IL-22 by RORγt$^+$ ILC3s without impacting the proportions of ILC3 subpopulations in the colonic LP.[10] Depletion of ILCs in *Rag*$^{-/-}$ mice using anti-CD90 antibody abrogated the Clostridia-induced reduction in intestinal permeability to food proteins. In this article, we examined the role of AhR in RORγt$^+$ cells in regulating intestinal permeability to food proteins and allergic responses to food. We showed that AhR expression by RORγt$^+$ cells was essential for the induction of IL-22 production by flagella. Neither Fla-C nor Fla-ST induced IL-22 production in the absence of functional AhR in RORγt$^+$ cells. Deletion of AhR specifically in RORγt$^+$ cells not only impaired IL-22 production and increased barrier permeability

but also increased susceptibility to an allergic response to food. Activation of AhR is necessary for IL-22 induction by commensal flagella. AhR signaling may also impact an allergic response to food in a manner independent of the induction of a gut barrier-protective response. The absence of AhR in ILC3s leads to an increase in apoptosis.[36] AhR expression on both epithelial cells and regulatory T cells (Tregs) is also important for the induction, gut-homing, and anti-inflammatory function of intestinal Tregs.[48,49] Additional effects on immune cells could lead to downstream signals that are independent of IL-22 but that still impact allergic sensitization. Beyond AhR, the pregnane X receptor (PXR), which also senses tryptophan metabolites, may contribute to the barrier-protective effect that we observe.[50]

In conclusion, our results have identified two groups of bacterial metabolites that contribute to the allergy protective effect of the Clostridia consortium beyond the actions of butyrate.[31] Flagella produced by these bacteria induced IL-22 in a manner dependent on AhR signaling in RORγt^+ cells and was barrier protective. The AhR ligand indole, which was also produced by the Clostridia consortium seems to have barrier-protective effects that are unrelated to IL-22 induction. Finally, mice lacking AhR signaling in RORγt^+ cells have impaired intestinal barrier function and were more susceptible to an allergic response to food.

Limitations of the study

The data presented in this study confirm and extend a previous report that revealed that a Clostridia-induced IL-22-dependent barrier-protective response was required for protection against allergic sensitization to food.[10] In this article, we examined whether there are other Clostridia-derived products and metabolites, in addition to butyrate, that induce an IL-22-dependent barrier-protective response. We examined the contributions of Clostridial production of flagella and indoles to epithelial barrier integrity. This analysis is not, however, exhaustive and does not exclude the potential influence of other AhR ligands or other, unrelated microbial products. We also cannot exclude the contributions of AhR or TLR5 signaling to protection against an allergic response to food that are independent of the induction of a gut barrier-protective response.

STAR★METHODS

RESOURCE AVAILABILITY

Lead contact—Further information and requests for resources and reagents should be directed to and will be fulfilled by the lead contact, Cathryn R. Nagler (cnagler@bsd.uchicago.edu).

Materials availability—Several bacterial strains were isolated during this study and are listed in the key resources table. These and other materials are available upon request to the lead contact as indicated above. Sharing of these resources will follow all institutional and funding agency requirements.

Data and code availability

- The raw, original data that support the findings of this study are available in Data S1.
- This paper does not report original code.
- The shotgun metagenomic and whole genome sequence data presented in this study are publicly available in a dataset uploaded to the National Center for Biotechnology Information Sequence Read Archive (SRA) under the BioProject number PRJNA1002412 with accession numbers SRA: SRR25527211, SRR25527212, SRR25528655, SRR25528656, SRR25528657.

EXPERIMENTAL MODEL AND STUDY PARTICIPANT DETAILS

Mice—SPF WT C57BL/6J, *Cd11c*^{Cre},[53] *Myd88*$^{fl/fl}$,[54] *Tlr5*$^{fl/fl}$,[33] *Ahr*$^{fl/fl}$,[55] *Myd88*$^{-/-}$,[54] and *Tlr5*$^{-/-}$[56] mice were originally purchased from The Jackson Laboratory. *Rorgt*^{Cre} mice[51] were obtained from Y.-X. Fu. *Tlr4*$^{-/-}$ mice were described in an earlier report.[52] All mice were on the C57BL/6J background and were bred and housed at the University of Chicago SPF or Gnotobiotic Research Animal Facilities. All mice in both facilities were housed in cages containing autoclaved Teklad Pine Shavings (cat# 7088) with a 12-h light/dark cycle at a standard RT of 20°C–24°C. SPF mice were weaned at 21 days of age and were fed an irradiated, plant-based mouse chow (Envigo 2918) and acidified water for the first week post weaning before transfer to an automatic watering system. All mice were tagged with unique metal ear tags. Gnotobiotic mice were maintained as described.[8] Mice were bred GF in Trexler-style flexible film isolator housing units and, for colonization with the Clostridia consortium, transferred into a repository isolator and colonized as described below. The colonization status of each isolator was checked weekly by 16S rRNA PCR analysis of fecal samples paired with anaerobic and aerobic culturing. Each experiment was performed using littermates randomly distributed among experimental groups (equally distributing males and females among groups). The age of the mice at the beginning of the experiments as well as the specific time points for data or sample collection are indicated in the Figure Legends. All experiments were approved by and performed in accordance with the guidelines of the Institutional Biosafety and Animal Care and Use Committees of the University of Chicago.

METHOD DETAILS

Anaerobic culturing of consortium bacteria and lysate generation—The cecum and colon of two colonized repository mice were dissected and brought into the anaerobic chamber (Coy Vinyl Anaerobic Chamber with CAM-12 monitor). Once inside the chamber, the cecal and colon contents were removed from the tissue and homogenized in sterile, pre-reduced PBS containing 0.05% L-cysteine. The homogenized contents were passed through a 100μm filter to remove large particles and the flow through containing bacterial cells was saved as the final cell slurry. 25μL of this fresh slurry was inoculated into tubes containing 6mL of pre-reduced chopped meat plus glucose (CMG) broth (Anaerobe Systems) with seven replicates. Sterile, pre-reduced glycerol was added to the remaining fresh slurry to a final concentration of 25% glycerol and the slurry was aliquoted and frozen at −80°C. The primary cultures were grown anaerobically at 37°C for 24h to an average optical density at

600 nm (OD_{600}) of 0.9 and then stored at 4°C. The culture with the highest OD_{600} was used to inoculate the secondary culture, approximately 50 mL of culture across three replicates. The secondary culture was also grown anaerobically at 37°C for 24h to an average OD_{600} of 1.10. Approximately 5mL of both the primary and secondary cultures were set aside and diluted with glycerol to a 25% final concentration, aliquoted, and frozen at −80°C. These glycerol stocks were used to inoculate new CMG or yeast casitone fatty acids (YCFA) broth for subsequent experiments. The remainder of the primary and secondary cultures was pooled and centrifuged at 3000xg for 7min to pellet cells. Supernatant was removed and cells were resuspended in 25mL of sterile DMEM, then aliquoted into autoclaved Eppendorf tubes containing 0.1 mm diameter glass beads. Tubes were shaken at 30 bps for 4min using a Retsch MM 400 bead beater to lyse cells, and resulting lysates were stored at −20°C until use.

Microbial DNA extraction and shotgun metagenomic sequencing—Shotgun metagenomic sequencing of cultured anaerobes was done by the University of Chicago Duchossois Family Institute at their Microbiome Metagenomics Facility. DNA was extracted with the QIAamp PowerFecal Pro DNA Kit, then libraries to be sequenced using the Illumina NextSeq platform were generated with the QIAseq FX Library Kit. The sequencing was performed at the Functional Genomics Facility at the University of Chicago with the 2×150 Paired Ends reads cassette.

Metagenomic assembly and specific analysis of flagellin, indole and butyrate gene abundance—Demultiplexed and quality filtered reads were assembled using metaSPAdes,[57] and Kraken2[58] was used to assign taxonomic classifications and determine relative abundance statistics. Sequencing data was demultiplexed using Qiime2 version 2019.7.[59] Open reading frames for contigs were determined using Prokka[60] and Kraken2 taxonomy was mapped to translated gene calls. Using hmmscan[61] a protein domain-based search of the consortium was conducted using curated PFAM[62] hidden Markov models (HMMs) for microbial indole production and select utilization-related gene domains (*iaaM*: PF01593.25, *ipdC:* PF02775.22, PF00205.23, PF02776.19, *tnaA:* PF01212.22) and flagellin-related gene domains (*Flagellin C:* PF00700.22, *Flagellin N:* PF00669.21, *FliJ:* PF02050.17), and TIGRFAM[63] HMMs for the key enzymatic steps in the major microbial butyrate production pathways,[64] butyryl-CoA:acetate CoA-transferase (*but*: TIGR03948.1) and butyrate kinase (*buk*: TIGR02707.1). Resulting hits from hmmscan analysis with assigned taxonomy were then used to construct the Venn diagram of species which encode some combination of indole, flagellin, or butyrate-associated gene protein domains.

Agar motility assay—Glycerol stocks of the Clostridia consortium, consortium isolates, *B. uniformis, or R. bromii* were used to inoculate YCFA broth and grown overnight at 37°C in anaerobic conditions. Once turbid, the OD_{600} of each culture was measured and adjusted to 0.5 by dilution before using 50μL of this suspension to inoculate a 7mL YCFA secondary culture. After another overnight growth, an inoculation stick was dipped into the secondary cultures and stabbed into tubes containing pre-reduced YCFA with 0.175% agar as described in a previous study.[65] These tubes were incubated for 48 h at 37°C in anaerobic conditions before images were taken.

Butyrate production and quantification—Glycerol stocks of the Clostridia consortium or consortium isolates were used to inoculate YCFA broth and grown overnight at 37°C in anaerobic conditions. Once turbid, the OD_{600} of each culture was measured and adjusted to 0.5 by dilution before using 50μL of this suspension to inoculate a 7mL YCFA or CMG secondary culture. The secondary cultures were grown at 37°C under anaerobic conditions for 48h. Aliquots of secondary cultures were spun at 10,000xg for 5min to pellet cells and stored at −80°C for further analysis. Butyrate concentrations in culture supernatants were measured by HPLC UV-Vis.[31] Samples were derivatized using 3-nitrophenylhydrazine (NPH) at 0.02M and N-(3-dimethylaminopropyl)-N′-ethylcarbodiimide hydrochloride (EDC) at 0.25M prepared in 1:1 H_2O:acetonitrile solution. Culture supernatants were diluted 1:2 or 1:5 in 1:1 H_2O:acetonitrile, then diluted in equal volume NPH and EDC solutions (1:1:1, sample:NPH:EDC). 2-ethyl-butyric acid was used as an internal standard. Samples were derivatized for 30 min at 65°C, then transferred to HPLC vials for analysis. Samples were run on an Agilent 1290 UHPLC using a ThermoFisher Scientific C18 4.6 × 50mm, 1.8μm particle size column. The mobile phases used were A: MilliQ H_2O +0.1% formic acid, and B: acetonitrile +0.1% formic acid. The mobile phase flow rate was 0.5 mL/min and a 5.0μL injection volume was used. The following solvent gradient was used: 0.0min 15% solvent B, 100% solvent B at 3.5min, 100% solvent B at 6min, 15% solvent B at 6.5min. Butyrate concentration was quantified as peak area relative to the internal standard and interpolated to a standard curve.

Indole production and tryptophan metabolite panel—Glycerol stocks of the Clostridia consortium, consortium isolates, *B. uniformis,* or *R. bromii* were used to inoculate YCFA broth and grown overnight at 37°C under anaerobic conditions. Once turbid, the OD_{600} of each culture was measured and adjusted to 0.5 by dilution before using 50μL of this suspension to inoculate a 7mL YCFA secondary culture. The secondary cultures were grown at 37°C in anaerobic conditions for 48h before assay for indole production using Kovac's reagent. Relative abundance of tryptophan or indicated tryptophan metabolites in the feces of mice was performed by the University of Chicago Duchossois Family Institute at their Host-Microbe Metabolomics Facility with a panel that utilized ultra-performance liquid chromatography paired with triple quadrupole mass spectrometry (UPLC-QqQ LC-MS) of mouse fecal pellets.

Consortium spore preparation and colonization of mice—Spores were prepared for colonization as described in an earlier report.[66] A primary culture of the Clostridia consortium was inoculated into YCFA broth from frozen glycerol stocks and grown at 37°C under anaerobic conditions for 48h. The growth was then diluted 1:10 in sporulation medium (3% w/v trypticase peptone, 1% w/v $Na_2HPO_4 \cdot 7H_2O$, pH 7.4) and incubated for 5 days at 30°C in anaerobic conditions and with agitation at 180rpm. Following this incubation period, the cell suspension was heat shocked at 65°C for 1min and returned to incubation for another 3 days in the same conditions. Next, a chloroform extraction was performed.[10] Chloroform was added to the suspension to 3% w/v, mixed vigorously for 5min and incubated for 1h at 37°C while shaking to eliminate vegetative cells. After removal of chloroform by 10min of CO_2 percolation, the resulting spore-containing solution was used to colonize adult GF mice as repositories. Subsequent colonization was performed by

i.g. gavage of feces collected from the repository mice. A freshly voided fecal pellet was resuspended in 1mL of sterile PBS; 250μL of the fecal supernatant was administered to weanling GF mice.

Isolation of Clostridia species and whole genome sequencing—Glycerol stocks of the Clostridia consortium were used to initiate overnight cultures in YCFA broth. Once grown, cultures were serially diluted in YCFA and spread plated onto YCFA agar plates. Individual colonies were then selected, made into frozen glycerol stocks, and screened using the motility, TLR5 stimulation, indole production and butyrate production assays described above. Two isolates and two mixed cultures of particular interest were selected for whole genome sequencing by the UChicago Duchossois Family Institute. DNA was extracted with the QIAamp PowerFecal Pro DNA Kit and libraries to be sequenced using the Illumina NextSeq platform were generated with the QIAseq FX Library Kit. The sequencing was performed at the Functional Genomics Facility at UChicago. Whole genome assembly and annotation were performed using SPAdes,[67] prokka[60] and RAST[68] with assistance from PATRIC.[69] Further annotation and flagellin protein structure prediction was done using Phyre2.[70] Flagellin gene alignment was performed using T-Coffee[71] and figure generation was done in Jalview.[72] A 16S rRNA-based phylogenetic tree was generated for these isolates including some of the most closely related taxa by NCBI BLAST and more distantly related outgroup species. Sequence alignment for the tree was done using Clustal Omega[73] and the tree itself was generated using IQ-TREE.[74]

Mouse TLR5-HeK cell line—TLR5 activation by flagella was examined using a HeK-Blue mTLR5 reporter cell line (Invivogen); cell maintenance and reporter assays were performed according to the manufacturer's instructions. Total protein concentration in flagella preparations was measured using the BCA protein assay kit (ThermoFisher Scientific). Flagella preparations were added to the reporter line at varying concentrations as indicated in the Figure Legends.

Neonatal antibiotic treatment—For neonatal Abx treatment pups were gavaged once daily with 100μL of an Abx mixture containing 4 mg/ml Kanamycin, 0.35 mg/ml Gentamycin, 8500U/ml Colistin, 2.15 mg/ml Metronidazole and 0.45 mg/ml Vancomycin in PBS starting at 7 days pre-weaning.[10,75] In most experiments mice continued to receive Abx in the drinking water post weaning; all antibiotics were diluted 1:50 compared to the gavage cocktail (except for Vancomycin (0.5 mg/mL). For measurements of serum FITC-dextran at day 6 post weaning in Figures 3C and S3D Abx treatment was discontinued at weaning.

RNA extraction from whole tissue, lamina propria or intestinal epithelial cells —Whole colon or ileum (defined as the 10cm directly proximal to the cecum) tissues were first extracted, flushed with PBS and divided into longitudinal strips. For experiments analyzing gene expression in whole colon or ileum, these strips were placed directly into RNAlater (ThermoFisher Scientific) and stored at 4°C overnight before being transferred to −80°C until further use. For experiments examining gene expression in IECs or LP, the IECs were removed according to a previous protocol.[76] The tissue strips were washed in PBS, then incubated in 30mM EDTA and 1.5mM DTT in PBS on ice for 20min followed

by 10 min at 37°C in 30mM EDTA in PBS. IECs were then mechanically dislodged from the tissue by shaking for 30s. The tissue remaining following IEC release was either washed and placed directly into RNA later, or stimulated *in vitro* with Fla-ST, Clostridial lysates or indole before storage in RNA later at 4°C overnight, then −80°C until further use. This tissue with the IECs removed was denoted LP tissue for gene expression analysis, similar to what has been reported previously.[25] The dislodged IECs were pelleted (5min, 800×g) and resuspended in Trizol. To extract RNA, the LP or whole tissue from colon or ileum was transferred into safe lock tubes with 1mL Trizol along with one 5mm stainless steel bead per tube before being disrupted at 30bps for 2min using a Retsch MM 400. RNA from these disrupted tissues or from IECs in Trizol was then extracted using the PureLink RNA Mini Kit (Ambion/Invitrogen) according to manufacturer's recommendations.

qRT-PCR—Gene expression in IECs, LP or whole tissue from the colon or ileum was determined as described.[10] Extracted RNA was reverse transcribed using the iScript cDNA Synthesis kit (BioRad) according to manufacturer's recommendations. Quantitative real-time PCR was performed using the Quantinova Sybr Green PCR Kit (Qiagen) on a QuantStudio 3 Real-Time PCR System (ThermoFisher Scientific), with the standard run protocol recommended for the SYBR green mix using primers from various sources[77–83] as outlined in Table S1. Relative expression was calculated using the ΔΔCt method using HPRT as the housekeeping gene, and then normalized to the control group (GF or Abx-treated control mice).

Intestinal tissue explant culture—Whole colon and ileum (defined as the 10cm directly proximal of the cecum) was harvested from mice, rinsed with PBS, opened or cut into 2 or 3 strips longitudinally, and placed into pre-weighed tubes containing HBSS (Corning Cellgro) with 50μM 2-mercaptoethanol, 100U/ml or μg/ml Penicillin/Streptomycin, 0.25μg/ml Fungizone and 10μg/ml Gentamicin. Tissue weights were determined and whole tissue was transferred into DMEM (HyClone) containing 10mM HEPES, 50μM 2-mercaptoethanol, 100U/ml or μg/ml Penicillin/Streptomycin, 0.25μg/ml Fungizone, 10% FCS, 2mM L-Glutamine, 0.1mM non-essential amino acids and 1mM sodium pyruvate. Ileum tissue was incubated at 50 mg/ml and colon tissue at 100 mg/ml for 24 h at 37°C. For stimulation of explants, recombinant murine IL-23 (Invitrogen) was added at 10 ng/ml, *Salmonella enterica* serovar Typhimurium flagellin (Fla-ST) (Invivogen) at 1μg/ml and Clostridia consortium lysate diluted 1:50. Stimulation with Fla-C or indole was done with various doses as indicated in the Figure Legends.

ELISAs—Concentrations of selected cytokines and chemokines in explant culture, serum, or splenocyte restimulation supernatants were determined using the IL-22 (BioLegend), IL-6 (BioLegend), CXCL1 (BioLegend) and IL-13 (Invitrogen) ELISA kits according to manufacturer's recommendations. To measure Peanut (PN) specific serum IgE and IgG1 levels, Immulon 2HB Flat Bottom Microtiter Plates were coated overnight at 4°C with 40μg/ml PN in 100mM Bicarbonate/Carbonate coating buffer (pH 9.6). Wells were blocked at RT for 2h with 3% BSA in PBS before incubation with samples and standards in PBS with 1% BSA overnight at 4°C. Bound PN-specific antibody levels were detected using goat-*anti*-mouse IgG1-HRP (Southern Biotech), with TMB as substrate, or unlabeled

goat-*anti*-mouse IgE (Southern Biotech) followed by rabbit anti-goat IgG-AP (Invitrogen), using *p*-NPP (KPL Labs) as substrate, and a SpectraMax M3 reader (Molecular Devices). A standard curve was used to quantify antibody concentrations. Standards were made in-house from the serum of PN-sensitized mice and purified using Protein G Sepharose followed by PN-coupled CNBr-Sepharose columns.[10] If needed, purified antibody solutions were concentrated using Amicon Ultra-4 30K Centrifugal filters (MilliporeSigma).

Isolation of flagella from commensal Clostridia—Two different preparation protocols were used to enrich for flagella in this study. The first was a more stringent enrichment done on the cultured consortium for use in *in vitro* explant stimulation and *in vivo* assays examining permeability to FITC-dextran (Figures 3 and S3). This method was based on a previous study isolating flagellin from *Campylobacter coli*[84] with various adjustments. Primary cultures of the consortium were inoculated into 7mL YCFA cultures using frozen glycerol stocks and left to grow at 37°C in anaerobic conditions for 48h. Each tube was then used to inoculate 500mL of YCFA media in an Erlenmeyer flask and incubated in the same conditions for 3 days. Following growth, the culture was transferred to a Ninja Professional 1000W blender model BL610 and blended on low setting for 2min. The suspension, not including the foam, was then centrifuged at 4200×g for 20min. The resulting supernatant was split into approximately 35mL aliquots in Ultra Clear centrifuge tubes (Beckman Coulter) and flagella were pelleted at 100,000×g for 1h in an Optima L-90k ultracentrifuge (Beckman Coulter). Following this, the pellet in each tube was resuspended in 1mL 25mM HEPES (pH 7.4) with 1% SDS, combined with other tubes and ultracentrifuged once again. The new pellets were resuspended in 1mL of 25mM HEPES (pH 7.4) and centrifuged twice at 10,000×g for another 20min before being filtered through a 0.22μm syringe filter. Total protein concentration for each prep was determined using a BCA protein assay kit (ThermoFisher Scientific) and examined for purity by Coomassie-stained SDS PAGE gel in addition to stimulation of the *in vitro* reporter cell line Hek-Blue mTLR5 (Invivogen). This preparation is referred to as Fla-C.

The second enrichment method was simpler and was used to test consortium isolates for TLR5 activation (Figure S1C). It was largely derived from a previous publication examining *Clostridioides difficile* flagellin[65] with some changes. YCFA agar plates were spread with 100μL of primary bacterial growth from YCFA overnight cultures and left to grow for 48h before being harvested and resuspended in 500μL. This suspension was transferred to a screw-capped microfuge tube and vortexed thoroughly for 5min before being centrifuged twice at 10,000×g for 20min. Total protein concentration of the collected supernatant was determined by BCA protein assay kit (ThermoFisher Scientific) and activation of TLR5 was examined using the *in vitro* reporter cell line Hek-Blue mTLR5 (Invivogen).

Flagellin injection—Mice were injected i.p. with 200μL/mouse of Fla-ST (Invivogen) or Fla-C in PBS at varying doses, as indicated in the Figure Legends. Negative control mice were i.p. injected with an equal amount of sterile PBS. Mice were injected either at weaning to measure IL-22 from colon and ileum explants harvested 2h post injection, or on days 1, 3 and 5 post weaning prior to assay for permeability to FITC-dextran on day 6. The concentration of CXCL1 and IL-6 was examined by ELISA using serum collected from

5–6-week old mice 2h after injection with 200μL/mouse of Fla-C (25 μg/mL) or Fla-ST (25 μg/mL)/PBS as reported previously.[30,33]

Intestinal permeability assay with FITC-dextran—To measure intestinal barrier permeability, mice were fasted for 3h before gavage of 500 mg/kg bodyweight 4kDa FITC-dextran.[85] Blood was collected in BD Microtainer SST Serum Tubes 90min or 2h post gavage (see Figure Legends) by cardiac bleed after CO_2 asphyxiation, allowed to clot for 30min and spun down for 7 min at 12,000×g. Serum was then diluted 1:3 in PBS and analyzed in duplicate using black polystyrene 96 well assay plates (Corning) and a SpectraMax M3 reader (Molecular Devices) with excitation at 485nm and detection at 528nm. Concentrations were determined using a standard curve of doubling dilutions of FITC-dextran in PBS with 1:3 normal mouse serum (NMS); 1:3 NMS in PBS was used as plate blank.

Treatment with indole and neutralizing anti-IL-22—Neonatal Abx-treated mice were gavaged i.g. once daily with 100μL of H_2O or indole (10 μg/mL) from weaning until 6 days post weaning before assessment of intestinal permeability on day 7 using the FITC-dextran assay. For experiments using IL-22 neutralizing antibodies, the mice were also i.p. injected with 150μL of either PBS, isotype control (1μg/μL, GP120 10E7.1D2, Genentech) or neutralizing anti-IL-22 antibody (1μg/μL, clone 8E11, Genentech) starting day 1 post weaning and continuing on days 3 and 5. In these experiments, daily H_2O or indole gavages ended on day 5 and the FITC-dextran assay was performed on day 6.

Preparation of peanut (PN) extract—PN extract was prepared from roasted, unsalted PN (Hampton Farms).[10,31] Shelled PN were ground in a food processor at 4°C to avoid overheating. The processed peanut was mixed with 20mM Tris-HCL (pH 7.2), using 1mL buffer per gram of PN, and incubated overnight at 4°C. The PN slurry was then separated by centrifugation at 4,000rpm for 30min, 4°C. The aqueous supernatant was collected and centrifuged again at 10,000rpm for 30min, 4°C. The supernatant from this centrifugation step was collected, sterile filtered through a Millipore ExpressPlus 0.22μm filter (MilliporeSigma) and the protein concentration of a diluted sample was determined by NanoDrop. Aliquots of PN extract were stored at −80°C and frozen aliquots were thawed for each experiment.

Allergic sensitization and challenge—Mice were sensitized using PN extract and cholera toxin (CT) followed by challenge with PN extract using a protocol adapted from previous publications.[10,75] Mice were sensitized weekly starting at weaning for 5 weeks (until day 28 post weaning). To reduce variability and improve allergen delivery, mice were fasted for 3h before gavage of 200mM sodium bicarbonate, followed 30min later by i.g. gavage of the sensitization dose of 6 mg PN extract and 10μg CT per mouse in a total volume of 150μL in 20mM Tris buffer (pH 7.2). On day 35 post weaning, mice were challenged by i.p. injection of 5 mg PN extract in 0.5mL PBS per mouse. Rectal temperatures were recorded pre-injection and every 15min following challenge, up to 90min post challenge. On day 42, mice received a second injection of 5 mg PN extract in 0.5 mL of PBS per mouse before euthanasia and blood collection on day 43.

Splenocyte isolation and restimulation—Spleens of sensitized mice were harvested on day 17 post weaning and processed with a 70μm cell strainer (ThermoFisher Scientific) before treatment with 2mL red blood cell lysis buffer (MilliporeSigma) for 10min on ice. Single cell suspensions were washed with complete RPMI and counted using a Countess II FL Automated Cell Counter (Invitrogen). Splenocytes were cultured in duplicate at 2×10^6 cells/ml in DMEM (HyClone) with 10mM HEPES, 50μM 2-mercaptoethanol, 100U/ml or μg/ml Penicillin/Streptomycin and 10% FCS with either 1 mg/ml defatted peanut powder (PB2, Bell Plantation, Inc.) or 1μg/ml anti-CD3/anti-CD28 for 72 h at 37°C.

Flow cytometry—Mesenteric lymph nodes (mLN) were digested for 30min using 0.5 mg/ml Collagenase D and 0.1 mg/ml DNAse in RPMI (Gibco) with 4% FCS before being strained through a 70μm cell strainer (ThermoFisher Scientific). Single cell suspensions were counted using a Countess II FL Automated Cell Counter (Invitrogen). Cells were stained using LIVE/DEAD Fixable Aqua Dead Cell Stain Kit (Invitrogen) for 15min before incubation with InVivoMAb anti-mouse CD16/CD32 for 10min and stained extracellularly with antibodies against CD3e, CD4, CD90.2 and lineage (or their isotype controls) for 30 min at room temperature. Cells were fixed and permeabilized using the eBioscience Foxp3/ Transcription Factor Staining Buffer Set (Invitrogen), followed by intracellular staining with antibodies against Foxp3 and RORγt (or their isotype controls) for 4–8h at 4°C. Cells were then resuspended in PBS with 1% BSA and acquired on an Attune NxT (ThermoFisher Scientific) flow cytometer. Data was analyzed using FlowJo v10.3 Software (BD Life Sciences).

QUANTIFICATION AND STATISTICAL ANALYSIS

Statistical analyses were performed using GraphPad Prism version 9.3.1. All data presented as concentration was log transformed before analysis. Comparisons of two groups were done by unpaired Student's t test, except for Figures 4B and 4C, which were paired analyses. Comparisons between more than two groups with treatment as the only variable were performed with one-way ANOVA with Tukey's or Dunnet's multiple comparisons tests. Comparisons between more than two groups with treatment and genotypes as variables were performed using two-way ANOVA using Sidak's multiple comparisons tests. Core body temperature differences were analyzed using unpaired Student's t test on the area under the curve values for each mouse.

Supplementary Material

Refer to Web version on PubMed Central for supplementary material.

ACKNOWLEDGMENTS

We thank the staff of The University of Chicago Gnotobiotic Research Facility for their expert technical support with gnotobiotic mouse experiments. We thank E. Littman and the Duchossois Family Institute for assistance with the microbiome analysis. We thank L. Maccio Maretto, S.M. Choi Hong, A. McFarland, and S. Cao for help with some experiments. This work was supported by the US National Institutes of Health grants R01 AI106302 and R01 AI146099. The graphical abstract was generated using BioRender.com.

INCLUSION AND DIVERSITY

We support inclusive, diverse, and equitable conduct of research.

REFERENCES

1. Sampath V, Abrams EM, Adlou B, Akdis C, Akdis M, Brough HA, Chan S, Chatchatee P, Chinthrajah RS, Cocco RR, et al. (2021). Food allergy across the globe. J. Allergy Clin. Immunol 148, 1347–1364. 10.1016/j.jaci.2021.10.018. [PubMed: 34872649]
2. Warren CM, Turner PJ, Chinthrajah RS, and Gupta RS (2021). Advancing Food Allergy Through Epidemiology: Understanding and Addressing Disparities in Food Allergy Management and Outcomes. J. Allergy Clin. Immunol. Pract 9, 110–118. 10.1016/j.jaip.2020.09.064. [PubMed: 33065370]
3. Brough HA, Lanser BJ, Sindher SB, Teng JMC, Leung DYM, Venter C, Chan SM, Santos AF, Bahnson HT, Guttman-Yassky E, et al. (2022). Early intervention and prevention of allergic diseases. Allergy 77, 416–441. 10.1111/all.15006. [PubMed: 34255344]
4. Iweala OI, and Nagler CR (2019). The Microbiome and Food Allergy. Annu. Rev. Immunol 37, 377–403. 10.1146/annurev-immunol-042718-041621. [PubMed: 31026410]
5. Bä ckhed F, Roswall J, Peng Y, Feng Q, Jia H, Kovatcheva-Datchary P, Li Y, Xia Y, Xie H, Zhong H, et al. (2015). Dynamics and Stabilization of the Human Gut Microbiome during the First Year of Life. Cell Host Microbe 17, 852. 10.1016/j.chom.2015.05.012. [PubMed: 26308884]
6. Al Nabhani Z, and Eberl G. (2020). Imprinting of the immune system by the microbiota early in life. Mucosal Immunol. 13, 183–189. 10.1038/s41385-020-0257-y. [PubMed: 31988466]
7. Torow N, Hand TW, and Hornef MW (2023). Programmed and environmental determinants driving neonatal mucosal immune development. Immunity 56, 485–499. 10.1016/j.immuni.2023.02.013. [PubMed: 36921575]
8. Feehley T, Plunkett CH, Bao R, Choi Hong SM, Culleen E, Belda-Ferre P, Campbell E, Aitoro R, Nocerino R, Paparo L, et al. (2019). Healthy infants harbor intestinal bacteria that protect against food allergy. Nat. Med 25, 448–453. 10.1038/s41591-018-0324-z. [PubMed: 30643289]
9. Bao R, Hesser LA, He Z, Zhou X, Nadeau KC, and Nagler CR (2021). Fecal microbiome and metabolome differ in healthy and food-allergic twins. J. Clin. Invest 131, e141935. 10.1172/JCI141935.
10. Stefka AT, Feehley T, Tripathi P, Qiu J, McCoy K, Mazmanian SK, Tjota MY, Seo GY, Cao S, Theriault BR, et al. (2014). Commensal bacteria protect against food allergen sensitization. Proc. Natl. Acad. Sci. USA 111, 13145–13150. 10.1073/pnas.1412008111. [PubMed: 25157157]
11. Aparicio-Domingo P, Romera-Hernandez M, Karrich JJ, Cornelissen F, Papazian N, Lindenbergh-Kortleve DJ, Butler JA, Boon L, Coles MC, Samsom JN, and Cupedo T. (2015). Type 3 innate lymphoid cells maintain intestinal epithelial stem cells after tissue damage. J. Exp. Med 212, 1783–1791. 10.1084/jem.20150318. [PubMed: 26392223]
12. Lindemans CA, Calafiore M, Mertelsmann AM, O'Connor MH, Dudakov JA, Jenq RR, Velardi E, Young LF, Smith OM, Lawrence G, et al. (2015). Interleukin-22 promotes intestinal-stem-cell-mediated epithelial regeneration. Nature 528, 560–564. 10.1038/nature16460. [PubMed: 26649819]
13. Gronke K, Herná ndez PP, Zimmermann J, Klose CSN, Kofoed-Branzk M, Guendel F, Witkowski M, Tizian C, Amann L, Schumacher F, et al. (2019). Interleukin-22 protects intestinal stem cells against genotoxic stress. Nature 566, 249–253. 10.1038/s41586-019-0899-7. [PubMed: 30700914]
14. Goto Y, Obata T, Kunisawa J, Sato S, Ivanov II, Lamichhane A, Takeyama N, Kamioka M, Sakamoto M, Matsuki T, et al. (2014). Innate lymphoid cells regulate intestinal epithelial cell glycosylation. Science 345, 1254009. 10.1126/science.1254009.
15. Pickard JM, Maurice CF, Kinnebrew MA, Abt MC, Schenten D, Golovkina TV, Bogatyrev SR, Ismagilov RF, Pamer EG, Turnbaugh PJ, and Chervonsky AV (2014). Rapid fucosylation of intestinal epithelium sustains host-commensal symbiosis in sickness. Nature 514, 638–641. 10.1038/nature13823. [PubMed: 25274297]

16. Sugimoto K, Ogawa A, Mizoguchi E, Shimomura Y, Andoh A, Bhan AK, Blumberg RS, Xavier RJ, and Mizoguchi A. (2008). IL-22 ameliorates intestinal inflammation in a mouse model of ulcerative colitis. J. Clin. Invest 118, 534–544. 10.1172/JCI33194. [PubMed: 18172556]

17. Zheng Y, Valdez PA, Danilenko DM, Hu Y, Sa SM, Gong Q, Abbas AR, Modrusan Z, Ghilardi N, de Sauvage FJ, and Ouyang W. (2008). Interleukin-22 mediates early host defense against attaching and effacing bacterial pathogens. Nat. Med 14, 282–289. 10.1038/nm1720. [PubMed: 18264109]

18. Sonnenberg GF, Monticelli LA, Alenghat T, Fung TC, Hutnick NA, Kunisawa J, Shibata N, Grunberg S, Sinha R, Zahm AM, et al. (2012). Innate lymphoid cells promote anatomical containment of lymphoid-resident commensal bacteria. Science 336, 1321–1325. 10.1126/science.1222551. [PubMed: 22674331]

19. Zelante T, Iannitti RG, Cunha C, De Luca A, Giovannini G, Pieraccini G, Zecchi R, D'Angelo C, Massi-Benedetti C, Fallarino F, et al. (2013). Tryptophan catabolites from microbiota engage aryl hydrocarbon receptor and balance mucosal reactivity via interleukin-22. Immunity 39, 372–385. 10.1016/j.immuni.2013.08.003. [PubMed: 23973224]

20. Chun E, Lavoie S, Fonseca-Pereira D, Bae S, Michaud M, Hoveyda HR, Fraser GL, Gallini Comeau CA, Glickman JN, Fuller MH, et al. (2019). Metabolite-Sensing Receptor Ffar2 Regulates Colonic Group 3 Innate Lymphoid Cells and Gut Immunity. Immunity 51, 871–884.e6. 10.1016/j.immuni.2019.09.014. [PubMed: 31628054]

21. Satpathy AT, Briseñ o CG, Lee JS, Ng D, Manieri NA, Kc W, Wu X, Thomas SR, Lee WL, Turkoz M, et al. (2013). Notch2-dependent classical dendritic cells orchestrate intestinal immunity to attaching-and-effacing bacterial pathogens. Nat. Immunol 14, 937–948. 10.1038/ni.2679. [PubMed: 23913046]

22. Longman RS, Diehl GE, Victorio DA, Huh JR, Galan C, Miraldi ER, Swaminath A, Bonneau R, Scherl EJ, and Littman DR (2014). CX(3)CR1(+) mononuclear phagocytes support colitis-associated innate lymphoid cell production of IL-22. J. Exp. Med 211, 1571–1583. 10.1084/jem.20140678. [PubMed: 25024136]

23. Arnold IC, Mathisen S, Schulthess J, Danne C, Hegazy AN, and Powrie F. (2016). CD11c(+) monocyte/macrophages promote chronic Helicobacter hepaticus-induced intestinal inflammation through the production of IL-23. Mucosal Immunol. 9, 352–363. 10.1038/mi.2015.65. [PubMed: 26242598]

24. Mao K, Baptista AP, Tamoutounour S, Zhuang L, Bouladoux N, Martins AJ, Huang Y, Gerner MY, Belkaid Y, and Germain RN (2018). Innate and adaptive lymphocytes sequentially shape the gut microbiota and lipid metabolism. Nature 554, 255–259. 10.1038/nature25437. [PubMed: 29364878]

25. Kinnebrew MA, Buffie CG, Diehl GE, Zenewicz LA, Leiner I, Hohl TM, Flavell RA, Littman DR, and Pamer EG (2012). Interleukin 23 production by intestinal CD103(+)CD11b(+) dendritic cells in response to bacterial flagellin enhances mucosal innate immune defense. Immunity 36, 276–287. 10.1016/j.immuni.2011.12.011. [PubMed: 22306017]

26. Hayashi F, Smith KD, Ozinsky A, Hawn TR, Yi EC, Goodlett DR, Eng JK, Akira S, Underhill DM, and Aderem A. (2001). The innate immune response to bacterial flagellin is mediated by Toll-like receptor 5. Nature 410, 1099–1103. 10.1038/35074106. [PubMed: 11323673]

27. Nakamura S, and Minamino T. (2019). Flagella-Driven Motility of Bacteria. Biomolecules 9, 279. 10.3390/biom9070279. [PubMed: 31337100]

28. Neville BA, Sheridan PO, Harris HMB, Coughlan S, Flint HJ, Duncan SH, Jeffery IB, Claesson MJ, Ross RP, Scott KP, and O'Toole PW (2013). Pro-inflammatory flagellin proteins of prevalent motile commensal bacteria are variably abundant in the intestinal microbiome of elderly humans. PLoS One 8, e68919. 10.1371/journal.pone.0068919.

29. Cullender TC, Chassaing B, Janzon A, Kumar K, Muller CE, Werner JJ, Angenent LT, Bell ME, Hay AG, Peterson DA, et al. (2013). Innate and adaptive immunity interact to quench microbiome flagellar motility in the gut. Cell Host Microbe 14, 571–581. 10.1016/j.chom.2013.10.009. [PubMed: 24237702]

30. Clasen SJ, Bell MEW, Borbó n A, Lee DH, Henseler ZM, de la Cuesta-Zuluaga J, Parys K, Zou J, Wang Y, Altmannova V, et al. (2023). Silent recognition of flagellins from human gut commensal bacteria by Toll-like receptor 5. Sci. Immunol 8, eabq7001. 10.1126/sciimmunol.abq7001.

31. Wang R, Cao S, Bashir MEH, Hesser LA, Su Y, Hong SMC, Thompson A, Culleen E, Sabados M, Dylla NP, et al. (2023). Treatment of peanut allergy and colitis in mice via the intestinal release of butyrate from polymeric micelles. Nat. Biomed. Eng 7, 38–55. 10.1038/s41551-022-00972-5. [PubMed: 36550307]
32. Kinnebrew MA, Ubeda C, Zenewicz LA, Smith N, Flavell RA, and Pamer EG (2010). Bacterial flagellin stimulates Toll-like receptor 5-dependent defense against vancomycin-resistant Enterococcus infe tion. J. Infect. Dis 201, 534–543. 10.1086/650203. [PubMed: 20064069]
33. Chassaing B, Ley RE, and Gewirtz AT (2014). Intestinal epithelial cell toll-like receptor 5 regulates the intestinal microbiota to prevent low-grade inflammation and metabolic syndrome in mice. Gastroenterology 147, 1363–1377.e17. 10.1053/j.gastro.2014.08.033. [PubMed: 25172014]
34. Steimle A, Menz S, Bender A, Ball B, Weber ANR, Hagemann T, Lange A, Maerz JK, Parusel R, Michaelis L, et al. (2019). Flagellin hypervariable region determines symbiotic properties of commensal Escherichia coli strains. PLoS Biol. 17, e3000334. 10.1371/journal.pbio.3000334.
35. Smith KD, Andersen-Nissen E, Hayashi F, Strobe K, Bergman MA, Barrett SLR, Cookson BT, and Aderem A. (2003). Toll-like receptor 5 recognizes a conserved site on flagellin required for protofilament formation and bacterial motility. Nat. Immunol 4, 1247–1253. 10.1038/ni1011. [PubMed: 14625549]
36. Qiu J, Heller JJ, Guo X, Chen Z.m.E., Fish K, Fu YX, and Zhou L. (2012). The aryl hydrocarbon receptor regulates gut immunity through modulation of innate lymphoid cells. Immunity 36, 92–104. 10.1016/j.immuni.2011.11.011. [PubMed: 22177117]
37. He YW, Beers C, Deftos ML, Ojala EW, Forbush KA, and Bevan MJ (2000). Down-regulation of the orphan nuclear receptor ROR gamma t is essential for T lymphocyte maturation. J. Immunol 164, 5668–5674. 10.4049/jimmunol.164.11.5668. [PubMed: 10820242]
38. Wang R, Xie H, Huang Z, Ma J, Fang X, Ding Y, and Sun Z. (2011). T cell factor 1 regulates thymocyte survival via a RORgammat-dependent pathway. J. Immunol 187, 5964–5973. 10.4049/jimmunol.1101205. [PubMed: 22039299]
39. Stockinger B, Shah K, and Wincent E. (2021). AHR in the intestinal microenvironment: safeguarding barrier function. Nat. Rev. Gastroenterol. Hepatol 18, 559–570. 10.1038/s41575-021-00430-8. [PubMed: 33742166]
40. Zenewicz LA, and Flavell RA (2008). IL-22 and inflammation: leukin' through a glass onion. Eur. J. Immunol 38, 3265–3268. 10.1002/eji.200838655. [PubMed: 19016525]
41. Zenewicz LA, Yancopoulos GD, Valenzuela DM, Murphy AJ, Stevens S, and Flavell RA (2008). Innate and adaptive interleukin-22 protects mice from inflammatory bowel disease. Immunity 29, 947–957. 10.1016/j.immuni.2008.11.003. [PubMed: 19100701]
42. Eken A, Singh AK, Treuting PM, and Oukka M. (2014). IL-23R+ innate lymphoid cells induce colitis via interleukin-22-dependent mechanism. Mucosal Immunol. 7, 143–154. 10.1038/mi.2013.33. [PubMed: 23715173]
43. Hu D, and Reeves PR (2020). The Remarkable Dual-Level Diversity of Prokaryotic Flagellins. mSystems 5, e00705–19-e00719. 10.1128/mSystems.00705-19.
44. Price AE, Shamardani K, Lugo KA, Deguine J, Roberts AW, Lee BL, and Barton GM (2018). A Map of Toll-like Receptor Expression in the Intestinal Epithelium Reveals Distinct Spatial, Cell Type-Specific, and Temporal Patterns. Immunity 49, 560–575.e6. 10.1016/j.immuni.2018.07.016. [PubMed: 30170812]
45. Kiss EA, Vonarbourg C, Kopfmann S, Hobeika E, Finke D, Esser C, and Diefenbach A. (2011). Natural aryl hydrocarbon receptor ligands control organogenesis of intestinal lymphoid follicles. Science 334, 1561–1565. 10.1126/science.1214914. [PubMed: 22033518]
46. Lee JS, Cella M, McDonald KG, Garlanda C, Kennedy GD, Nukaya M, Mantovani A, Kopan R, Bradfield CA, Newberry RD, and Colonna M. (2011). AHR drives the development of gut ILC22 cells and postnatal lymphoid tissues via pathways dependent on and independent of Notch. Nat. Immunol 13, 144–151. 10.1038/ni.2187. [PubMed: 22101730]
47. Qiu J, Guo X, Chen ZME, He L, Sonnenberg GF, Artis D, Fu YX, and Zhou L. (2013). Group 3 innate lymphoid cells inhibit T-cell-mediated intestinal inflammation through aryl hydrocarbon receptor signaling and regulation of microflora. Immunity 39, 386–399. 10.1016/j.immuni.2013.08.002. [PubMed: 23954130]

48. Yoshimatsu Y, Sujino T, Miyamoto K, Harada Y, Tanemoto S, Ono K, Umeda S, Yoshida K, Teratani T, Suzuki T, et al. (2022). Aryl hydrocarbon receptor signals in epithelial cells govern the recruitment and location of Helios(+) Tregs in the gut. Cell Rep. 39, 110773. 10.1016/j.celrep.2022.110773.
49. Ye J, Qiu J, Bostick JW, Ueda A, Schjerven H, Li S, Jobin C, Chen ZME, and Zhou L. (2017). The Aryl Hydrocarbon Receptor Preferentially Marks and Promotes Gut Regulatory T Cells. Cell Rep. 21, 2277–2290. 10.1016/j.celrep.2017.10.114. [PubMed: 29166616]
50. Venkatesh M, Mukherjee S, Wang H, Li H, Sun K, Benechet AP, Qiu Z, Maher L, Redinbo MR, Phillips RS, et al. (2014). Symbiotic bacterial metabolites regulate gastrointestinal barrier function via the xenobiotic sensor PXR and Toll-like receptor 4. Immunity 41, 296–310. 10.1016/j.immuni.2014.06.014. [PubMed: 25065623]
51. Eberl G, and Littman DR (2004). Thymic origin of intestinal alphabeta T cells revealed by fate mapping of RORgammat+ cells. Science 305, 248–251. 10.1126/science.1096472. [PubMed: 15247480]
52. Matharu KS, Mizoguchi E, Cotoner CA, Nguyen DD, Mingle B, Iweala OI, McBee ME, Stefka AT, Prioult G, Haigis KM, et al. (2009). Toll-like receptor 4-mediated regulation of spontaneous Helicobacter-dependent colitis in IL-10-deficient mice. Gastroenterology 137, 1380–1390.e1–3. 10.1053/j.gastro.2009.07.004. [PubMed: 19596011]
53. Caton ML, Smith-Raska MR, and Reizis B. (2007). Notch-RBP-J signaling controls the homeostasis of CD8- dendritic cells in the spleen. J. Exp. Med 204, 1653–1664. 10.1084/jem.20062648. [PubMed: 17591855]
54. Hou B, Reizis B, and DeFranco AL (2008). Toll-like receptors activate innate and adaptive immunity by using dendritic cell-intrinsic and -extrinsic mechanisms. Immunity 29, 272–282. 10.1016/j.immuni.2008.05.016. [PubMed: 18656388]
55. Walisser JA, Glover E, Pande K, Liss AL, and Bradfield CA (2005). Aryl hydrocarbon receptor-dependent liver development and hepatotoxicity are mediated by different cell types. Proc. Natl. Acad. Sci. USA 102, 17858–17863. 10.1073/pnas.0504757102. [PubMed: 16301529]
56. Feuillet V, Medjane S, Mondor I, Demaria O, Pagni PP, Galán JE, Flavell RA, and Alexopoulou L. (2006). Involvement of Toll-like receptor 5 in the recognition of flagellated bacteria. Proc. Natl. Acad. Sci. USA 103, 12487–12492. 10.1073/pnas.0605200103. [PubMed: 16891416]
57. Nurk S, Meleshko D, Korobeynikov A, and Pevzner PA (2017). meta-SPAdes: a new versatile metagenomic assembler. Genome Res. 27, 824–834. 10.1101/gr.213959.116. [PubMed: 28298430]
58. Wood DE, Lu J, and Langmead B. (2019). Improved metagenomic analysis with Kraken 2. Genome Biol. 20, 257. 10.1186/s13059-019-1891-0. [PubMed: 31779668]
59. Bolyen E, Rideout JR, Dillon MR, Bokulich NA, Abnet CC, Al-Ghalith GA, Alexander H, Alm EJ, Arumugam M, Asnicar F, et al. (2019). Reproducible, interactive, scalable and extensible microbiome data science using QIIME 2. Nat. Biotechnol 37, 852–857. 10.1038/s41587-019-0209-9. [PubMed: 31341288]
60. Seemann T. (2014). Prokka: rapid prokaryotic genome annotation. Bioinformatics 30, 2068–2069. 10.1093/bioinformatics/btu153. [PubMed: 24642063]
61. Potter SC, Luciani A, Eddy SR, Park Y, Lopez R, and Finn RD (2018). HMMER web server: 2018 update. Nucleic Acids Res. 46, W200–W204. 10.1093/nar/gky448. [PubMed: 29905871]
62. El-Gebali S, Mistry J, Bateman A, Eddy SR, Luciani A, Potter SC, Qureshi M, Richardson LJ, Salazar GA, Smart A, et al. (2019). The Pfam protein families database in 2019. Nucleic Acids Res. 47, D427–D432. 10.1093/nar/gky995. [PubMed: 30357350]
63. Li W, O'Neill KR, Haft DH, DiCuccio M, Chetvernin V, Badretdin A, Coulouris G, Chitsaz F, Derbyshire MK, Durkin AS, et al. (2021). RefSeq: expanding the Prokaryotic Genome Annotation Pipeline reach with protein family model curation. Nucleic Acids Res. 49, D1020–D1028. 10.1093/nar/gkaa1105. [PubMed: 33270901]
64. Vital M, Howe AC, and Tiedje JM (2014). Revealing the bacterial butyrate synthesis pathways by analyzing (meta)genomic data. mBio 5, e00889. 10.1128/mBio.00889-14.
65. Twine SM, Reid CW, Aubry A, McMullin DR, Fulton KM, Austin J, and Logan SM (2009). Motility and flagellar glycosylation in Clostridium difficile. J. Bacteriol 191, 7050–7062. 10.1128/JB.00861-09. [PubMed: 19749038]

66. Yang WW, Crow-Willard EN, and Ponce A. (2009). Production and characterization of pure Clostridium spore suspensions. J. Appl. Micro-biol 106, 27–33. 10.1111/j.1365-2672.2008.03931.x.

67. Bankevich A, Nurk S, Antipov D, Gurevich AA, Dvorkin M, Kulikov AS, Lesin VM, Nikolenko SI, Pham S, Prjibelski AD, et al. (2012). SPAdes: a new genome assembly algorithm and its applications to single-cell sequencing. J. Comput. Biol 19, 455–477. 10.1089/cmb.2012.0021. [PubMed: 22506599]

68. Brettin T, Davis JJ, Disz T, Edwards RA, Gerdes S, Olsen GJ, Olson R, Overbeek R, Parrello B, Pusch GD, et al. (2015). RASTtk: a modular and extensible implementation of the RAST algorithm for building custom annotation pipelines and annotating batches of genomes. Sci. Rep 5, 8365. 10.1038/srep08365. [PubMed: 25666585]

69. Davis JJ, Wattam AR, Aziz RK, Brettin T, Butler R, Butler RM, Chlenski P, Conrad N, Dickerman A, Dietrich EM, et al. (2020). The PATRIC Bioinformatics Resource Center: expanding data and analysis capabilities. Nucleic Acids Res. 48, D606–D612. 10.1093/nar/gkz943. [PubMed: 31667520]

70. Kelley LA, Mezulis S, Yates CM, Wass MN, and Sternberg MJE (2015). The Phyre2 web portal for protein modeling, prediction and analysis. Nat. Protoc 10, 845–858. 10.1038/nprot.2015.053. [PubMed: 25950237]

71. Madeira F, Park YM, Lee J, Buso N, Gur T, Madhusoodanan N, Basutkar P, Tivey ARN, Potter SC, Finn RD, and Lopez R. (2019). The EMBL-EBI search and sequence analysis tools APIs in 2019. Nucleic Acids Res. 47, W636–W641. 10.1093/nar/gkz268. [PubMed: 30976793]

72. Waterhouse AM, Procter JB, Martin DMA, Clamp M, and Barton GJ (2009). Jalview Version 2--a multiple sequence alignment editor and analysis workbench. Bioinformatics 25, 1189–1191. 10.1093/bioinformatics/btp033. [PubMed: 19151095]

73. Sievers F, Wilm A, Dineen D, Gibson TJ, Karplus K, Li W, Lopez R, McWilliam H, Remmert M, Sö ding J, et al. (2011). Fast, scalable generation of high-quality protein multiple sequence alignments using Clustal Omega. Mol. Syst. Biol 7, 539. 10.1038/msb.2011.75. [PubMed: 21988835]

74. Nguyen LT, Schmidt HA, von Haeseler A, and Minh BQ (2015). IQ-TREE: a fast and effective stochastic algorithm for estimating maximum-likelihood phylogenies. Mol. Biol. Evol 32, 268–274. 10.1093/molbev/msu300. [PubMed: 25371430]

75. Bashir MEH, Louie S, Shi HN, and Nagler-Anderson C. (2004). Toll-like receptor 4 signaling by intestinal microbes influences susceptibility to food allergy. J. Immunol 172, 6978–6987. 10.4049/jimmunol.172.11.6978. [PubMed: 15153518]

76. Gracz AD, Puthoff BJ, and Magness ST (2012). Identification, isolation, and culture of intestinal epithelial stem cells from murine intestine. Methods Mol. Biol 879, 89–107. 10.1007/978-1-61779-815-3_6. [PubMed: 22610555]

77. Upadhyay V, Poroyko V, Kim TJ, Devkota S, Fu S, Liu D, Tumanov AV, Koroleva EP, Deng L, Nagler C, et al. (2012). Lymphotoxin regulates commensal responses to enable diet-induced obesity. Nat. Immunol 13, 947–953. 10.1038/ni.2403. [PubMed: 22922363]

78. Sugiura Y, Kamdar K, Khakpour S, Young G, Karpus WJ, and De-Paolo RW (2013). TLR1-induced chemokine production is critical for mucosal immunity against Yersinia enterocolitica. Mucosal Immunol. 6, 1101–1109. 10.1038/mi.2013.5. [PubMed: 23443468]

79. Wongchana W, Kongkavitoon P, Tangtanatakul P, Sittplangkoon C, Butta P, Chawalitpong S, Pattarakankul T, Osborne BA, and Palaga T. (2018). Notch signaling regulates the responses of lipopolysaccharide-stimulated macrophages in the presence of immune complexes. PLoS One 13, e0198609. 10.1371/journal.pone.0198609.

80. Kreymborg K, Etzensperger R, Dumoutier L, Haak S, Rebollo A, Buch T, Heppner FL, Renauld JC, and Becher B. (2007). IL-22 is expressed by Th17 cells in an IL-23-dependent fashion, but not required for the development of autoimmune encephalomyelitis. J. Immunol 179, 8098–8104. 10.4049/jimmunol.179.12.8098. [PubMed: 18056351]

81. Suhail A, Rizvi ZA, Mujagond P, Ali SA, Gaur P, Singh M, Ahuja V, Awasthi A, and Srikanth CV (2019). DeSUMOylase SENP7-Mediated Epithelial Signaling Triggers Intestinal Inflammation via Expansion of Gamma-Delta T Cells. Cell Rep. 29, 3522–3538.e7. 10.1016/j.celrep.2019.11.028. [PubMed: 31825833]

82. Miki T, Goto R, Fujimoto M, Okada N, and Hardt WD (2017). The Bactericidal Lectin RegIIIbeta Prolongs Gut Colonization and Enteropathy in the Streptomycin Mouse Model for Salmonella Diarrhea. Cell Host Microbe 21, 195–207. 10.1016/j.chom.2016.12.008. [PubMed: 28111202]

83. Wang L, Zhang K, Ding X, Wang Y, Bai H, Yang Q, Ben J, Zhang H, Li X, Chen Q, and Zhu X. (2020). Fucoidan antagonizes diet-induced obesity and inflammation in mice. J. Biomed. Res 35, 197–205. 10.7555/JBR.34.20200153. [PubMed: 33495425]

84. Power ME, Guerry P, McCubbin WD, Kay CM, and Trust TJ (1994). Structural and antigenic characteristics of Campylobacter coli FlaA flagellin. J. Bacteriol 176, 3303–3313. 10.1128/jb.176.11.3303-3313.1994. [PubMed: 7515043]

85. Cani PD, Possemiers S, Van de Wiele T, Guiot Y, Everard A, Rottier O, Geurts L, Naslain D, Neyrinck A, Lambert DM, et al. (2009). Changes in gut microbiota control inflammation in obese mice through a mechanism involving GLP-2-driven improvement of gut permeability. Gut 58, 1091–1103. 10.1136/gut.2008.165886. [PubMed: 19240062]

Highlights

- A consortium of Clostridia contains taxa that are flagellated and produce indole
- Induction of IL-22 by Clostridial flagella requires TLR5 signaling in $CD11c^+$ DCs
- Intestinal permeability is increased in mice with AhR deficiency in $ROR\gamma t^+$ ILC3s
- Clostridial products enhance barrier function to protect against food allergy

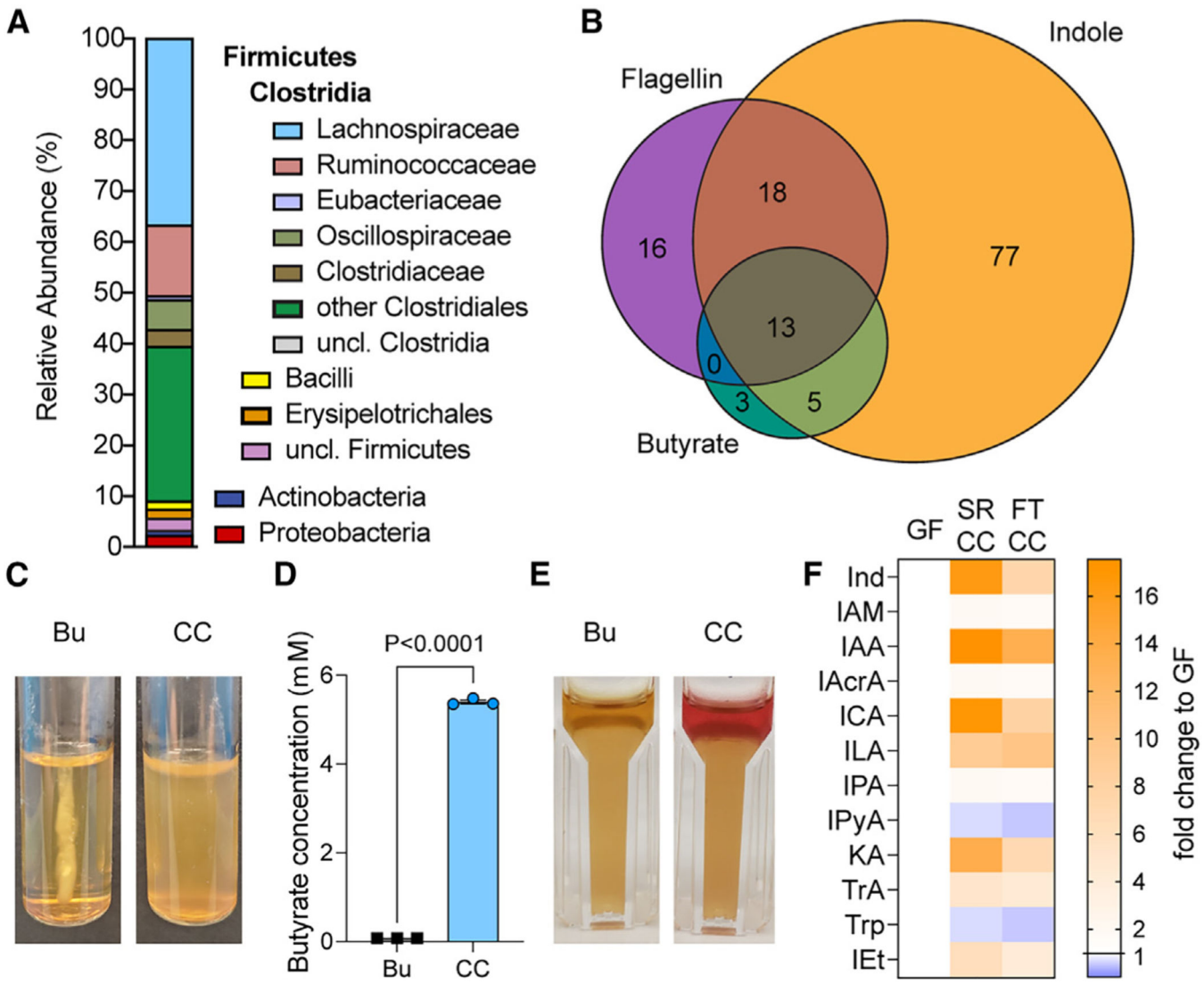

Figure 1. Taxa in the Clostridia consortium are flagellated and produce indole and butyrate

(A) The relative abundance of different taxa in the consortium after culturing as determined by shotgun metagenomic sequencing.

(B) A Venn diagram constructed from analysis of the cultured consortium shotgun metagenomic data denoting the number of species that encode some combination of the protein domains involved in the production of flagellin, indole, or butyrate.

(C) Representative images depicting the motility of negative control *Bacteroides uniformis* (Bu) and the cultured consortium (CC) away from a central inoculation stab in agar.

(D) Butyrate production by the cultured Clostridia consortium in CMG medium compared to Bu as quantified by HPLC UV-vis. Graph represents mean ± SEM and includes individual data points from separate cultures. Significance was determined using Student's t test after log transformation of data.

(E) Representative images showing production of indole by the addition of Kovac's reagent to the top of Bu or Clostridia consortium cultures.

(F) Relative abundance of tryptophan or indicated tryptophan metabolites in the feces of germ-free (GF) mice, mice colonized with spores from the Clostridia consortium cultures described in (A) (SRCC), or mice colonized by fecal transfer from SRCC mice (FTCC), normalized to amounts measured in GF feces (n = 3 mice per group). Ind, indole; IAM, indole 3′ acetamide; IAA, indole 3′ acetic acid; IAcrA, indole 3′ acrylic acid; ICA, indole 3′ carboxylic acid; ILA, indole 3′ lactic acid; IPA, indole 3′ propionic acid; IPyA, indole pyruvic acid; KA, kynurenic acid; TrA, tryptamine; Trp, tryptophan; IEt, indole 3′ ethanol. See also Figure S1.

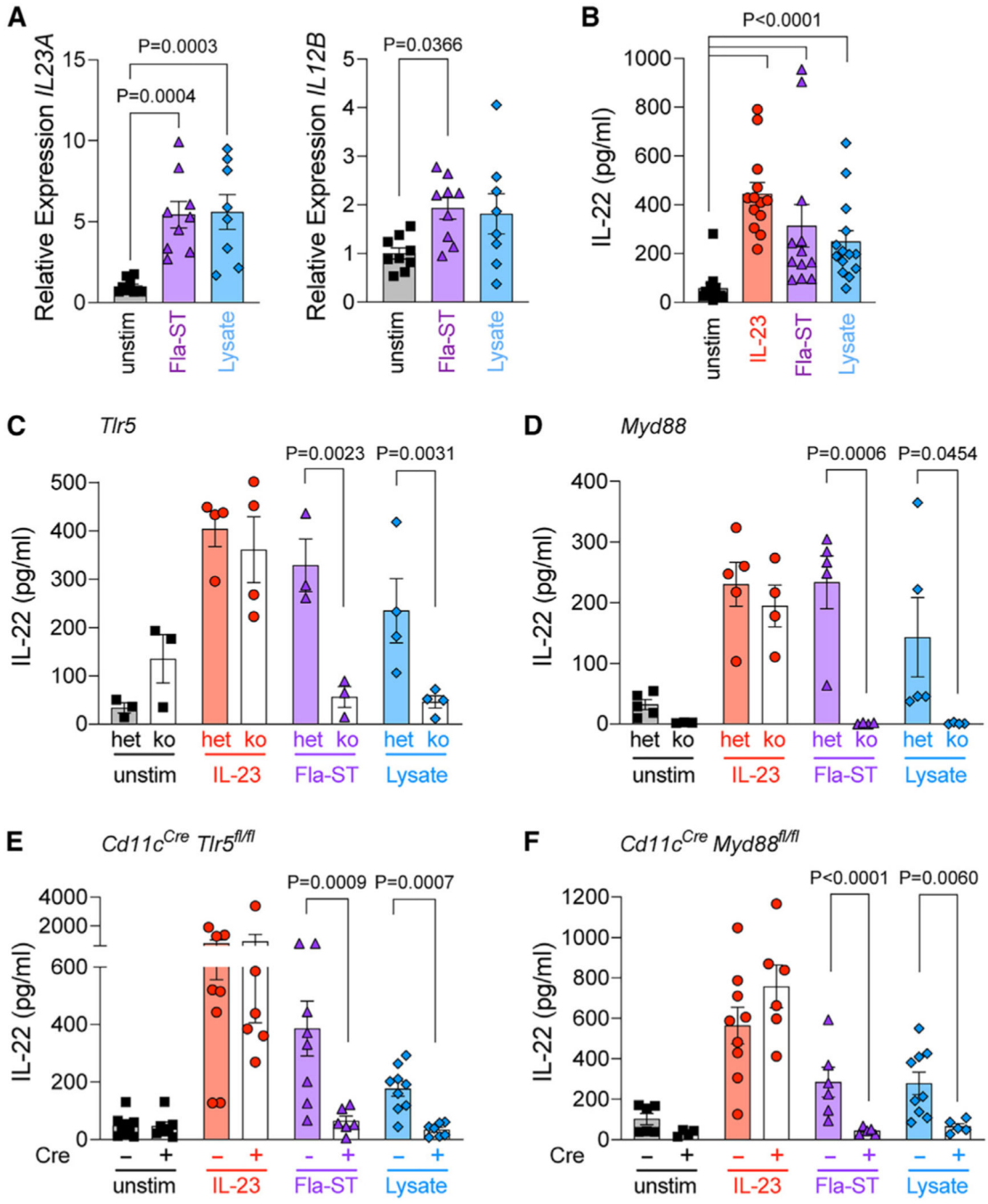

Figure 2. Clostridia lysates induce intestinal IL-22 through TLR5 and MyD88

(A) Transcript levels of both IL-23 subunits in ileal LP tissue from neonatal Abx-treated WT C57BL/6 mice harvested on day 7 post-weaning and stimulated *in vitro* with Fla-ST (1 μg/mL) or Clostridia lysate for 45 min. Data are pooled from 3 independent experiments (n = 10, 9, and 8).

(B) IL-22 production by ileum explants from neonatal Abx-treated C57BL/6 mice harvested on day 7 post-weaning and stimulated *in vitro* with IL-23 (10 ng/mL), Fla-ST (1 μg/mL), or

Clostridia lysate for 24 h. Data are pooled from 2 independent experiments (n = 13, 13, 12, and 14).

(C) IL-22 production by ileum explants from neonatal Abx-treated *Tlr5*$^{+/-}$ and *Tlr5*$^{-/-}$ mice harvested on day 7 post-weaning and stimulated *in vitro* with IL-23 (10 ng/mL), Fla-ST (1 μg/mL), or Clostridia lysate for 24 h. Data are pooled from 2 independent experiments (n = 3/3, 4/4, 3/3, and 4/4).

(D) IL-22 production by ileum explants from neonatal Abx-treated *Myd88*$^{+/-}$ and *Myd88*$^{-/-}$ mice harvested on day 7 post-weaning and stimulated *in vitro* with IL-23 (10 ng/mL), Fla-ST (1 μg/mL), or Clostridia lysate for 24 h. Data are pooled from 2 independent experiments (n = 5/3, 5/4, 5/4, and 5/4).

(E) IL-22 production by ileum explants from neonatal Abx-treated *Cd11c*^{Cre} *Tlr5*$^{fl/fl}$ and *Tlr5*$^{fl/fl}$ mice harvested on day 7 post-weaning and stimulated *in vitro* with IL-23 (10 ng/mL), Fla-ST (1 μg/mL), or Clostridia lysate for 24 h. Data are pooled from 3 independent experiments (n = 9/7, 8/6, 8/6, and 9/7).

(F) IL-22 production by ileum explants from neonatal Abx-treated *Cd11c*^{Cre} *Myd88* $^{fl/fl}$ and *Myd88* $^{fl/fl}$ mice harvested on day 7 post-weaning and stimulated *in vitro* with IL-23 (10 ng/mL), Fla-ST (1 μg/mL), or Clostridia lysate for 24 h. Data are pooled from 3 independent experiments (n = 6/4, 9/6, 6/5, and 9/5).

All graphs represent mean ± SEM and include individual data points. Significance was determined using one-way ANOVA with Tukey's multiple comparisons test (A and B) or two-way ANOVA with Sidak's multiple comparisons test (C–F) after log transformation of data (for B–F).

See also Figure S2.

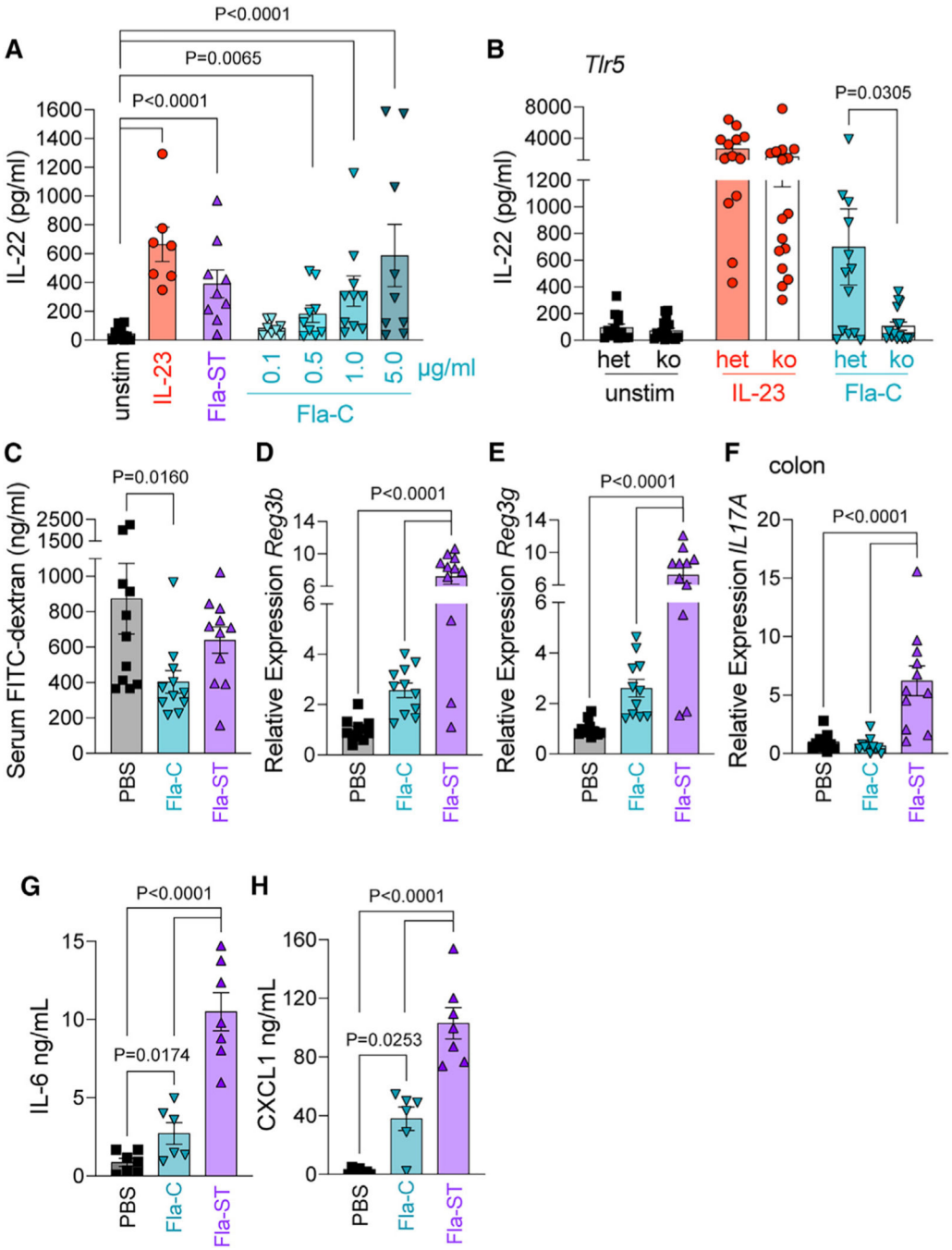

Figure 3. Commensal Clostridia flagella induce intestinal IL-22 and reduce barrier permeability *in vivo*

(A) IL-22 production by ileum explants from neonatal Abx-treated C57BL/6 mice harvested on day 7 post-weaning and stimulated *in vitro* with IL-23 (10 ng/mL), Fla-ST (1 µg/mL), or Fla-C as indicated for 24 h. Data are pooled from 2 independent experiments (n = 10, 7, 9, 8, 9, 10, and 9).

(B) IL-22 production by ileum explants from neonatal Abx-treated *Tlr5*$^{+/-}$ and *Tlr5*$^{-/-}$ mice harvested on day 7 post-weaning and stimulated *in vitro* with IL-23 (10 ng/mL) or Fla-C (5 µg/mL) for 24 h. Data are pooled from 3 independent experiments (n = 13 and 16).

(C) Serum FITC-dextran concentrations at euthanasia 2 h post-gavage on day 6 post-weaning from neonatal Abx-treated C57BL/6 mice injected i.p. with PBS, Fla-C (5 μg/injection), or Fla-ST (5 μg/injection) at days 1, 3, and 5 post-weaning. Data are pooled from 2 independent experiments (n = 11, 11, and 11).
(D) Transcript levels of *Reg3b* in ileal IECs from mice in (C), relative to PBS group.
(E) Transcript levels of *Reg3g* in ileal IECs from mice in (C), relative to PBS group.
(F) Transcript levels of *Il17a* in colon LP tissue from mice in (C), relative to PBS group.
(G) IL-6 concentration in serum from neonatal Abx-treated adult C57BL/6 mice collected 2 h after i.p. injection of PBS, Fla-C (5 μg), or Fla-ST (5 μg). Data are pooled from 2 independent experiments (n = 7, 6, and 7).
(H) CXCL1 concentration in serum from mice in (G). All bar graphs represent mean ± SEM and include individual data points. Significance was determined using one-way ANOVA with Dunnett's multiple comparisons test to compare all groups with the unstimulated control (A) or Tukey's multiple comparisons test to compare each group with one another (C–H). For (B), two-way ANOVA with Sidak's multiple comparisons test was used. Statistics for (A)–(C), (G), and (H) were performed after log transformation of data.
See also Figure S3.

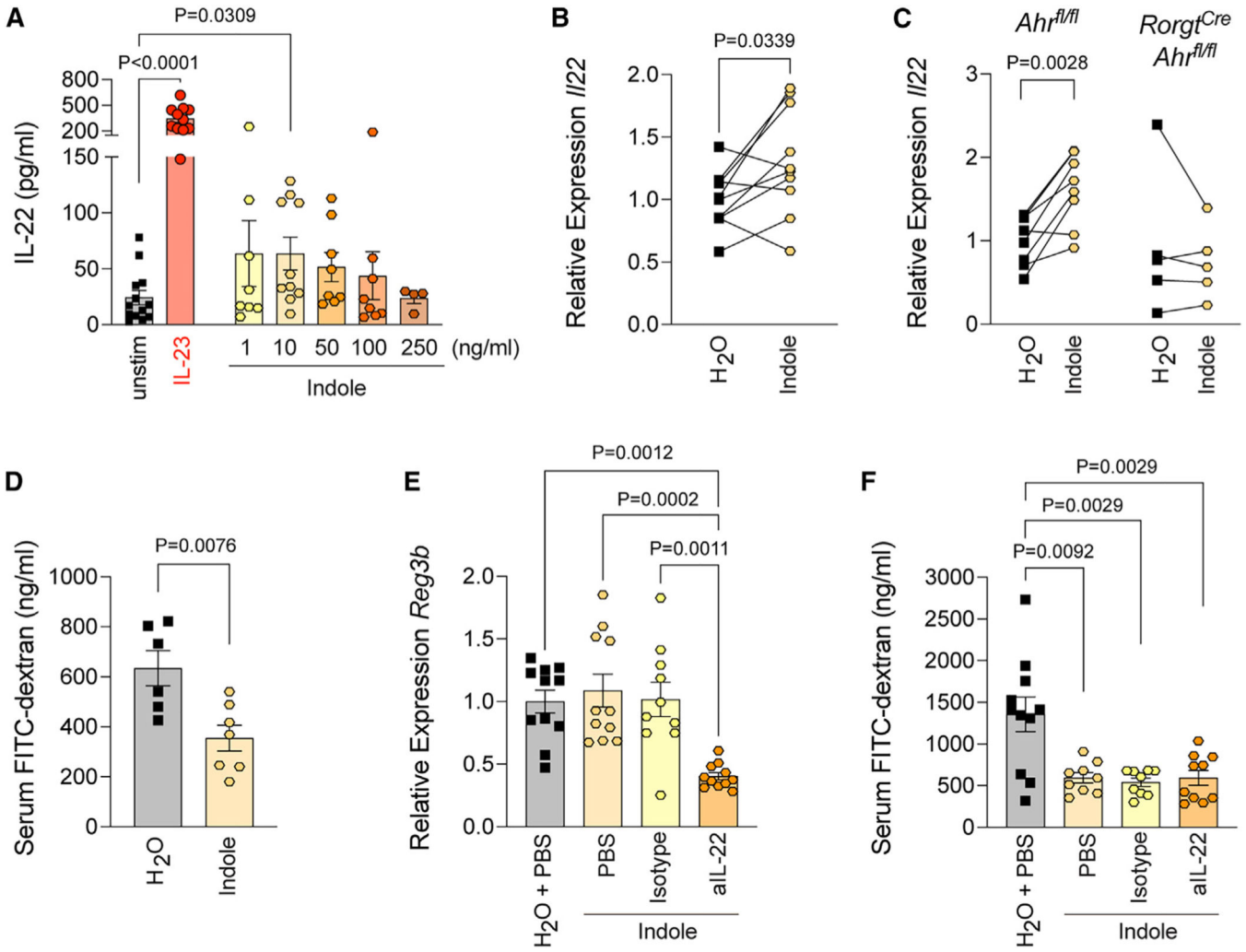

Figure 4. Indole has a barrier-protective effect independent of its induction of IL-22

(A) IL-22 production by ileum explants from neonatal Abx-treated C57BL/6 mice harvested on day 7 post-weaning and stimulated *in vitro* with IL-23 (10 ng/mL) or indole as indicated for 24 h. Data are pooled from 4 independent experiments (n = 13, 11, 8, 10, 8, 8, and 4).

(B) Transcript levels of *Il22* in ileum LP tissue from neonatal Abx-treated C57BL/6 mice harvested on day 7 post-weaning where half of each ileum was left untreated and the other half was stimulated with 10 ng/mL indole for 1 h. Data are pooled from 2 independent experiments (n = 10).

(C) Transcript levels of *Il22* in ileum LP tissue from neonatal Abx-treated *Rorgt*^{Cre} *Ahr*$^{fl/fl}$ mice and their *Ahr*$^{fl/fl}$ littermates harvested on day 7 post-weaning where half of each ileum was left untreated and the other half was stimulated with 10 ng/mL indole *in vitro* for 1 h. Data are pooled from 2 independent experiments (n = 10).

(D) Serum FITC-dextran concentrations at euthanasia 2 h post-gavage on day 7 post-weaning from neonatal Abx-treated C57BL/6 mice that were gavaged daily with 100 μL indole (10 μg/mL) or water starting at weaning until day 6. Data are pooled from 3 independent experiments (n = 6 and 7).

(E) Transcript levels of *Reg3b* in ileal IECs from neonatal Abx-treated mice that were gavaged daily with 100 μL indole (10 μg/mL) or water starting at weaning until day 5. PBS, isotype control antibody (150 μg), or anti-IL-22 antibody (150 μg) was injected i.p. on days 1, 3, and 5. Tissues were collected on day 6. Data are pooled from 2 independent experiments (n = 11, 11, 10, and 11).

(F) Serum FITC-dextran concentrations at euthanasia 2 h post-gavage on day 6 post-weaning of mice in (E).

All bar graphs represent mean ± SEM and include individual data points. (B) and (C) show individual data points where connecting lines indicate tissues from the same mouse. Significance was determined using one-way ANOVA with Dunnett's multiple comparisons test to compare all groups with the unstimulated control (A) or Tukey's multiple comparisons test to compare each group with one another (E and F). Student's t test was used (paired for B and C, unpaired for D) to determine significance for the remaining panels. Statistics for (A), (D), and (F) were performed after log transformation of data.

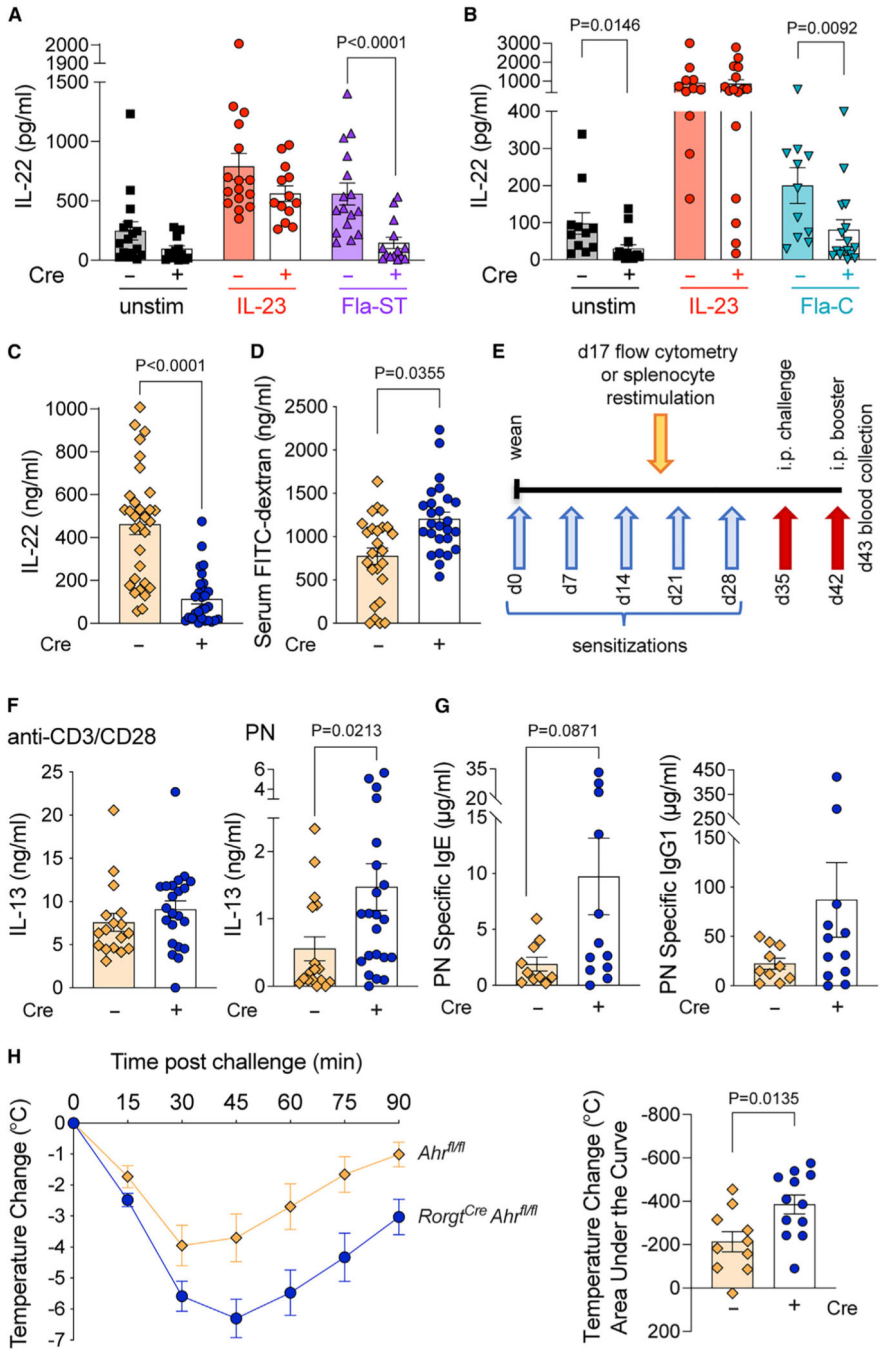

Figure 5. AhR signaling in RORγt$^+$ cells is necessary for IL-22 induction and protection against food allergies

(A) IL-22 production by ileum explants from neonatal Abx-treated *Rorgt^{Cre} Ahr$^{fl/fl}$* mice and their *Ahr$^{fl/fl}$* littermates harvested on day 7 post-weaning and stimulated *in vitro* with IL-23 (10 ng/mL) or Fla-ST (1 µg/mL) for 24 h. Data are pooled from 2 independent experiments (n = 16 and 14).

(B) IL-22 production by ileum explants from Abx-treated *Rorgt^{Cre} Ahr$^{fl/fl}$* mice and their *Ahr$^{fl/fl}$* littermates harvested on day 7 post-weaning and stimulated *in vitro* with IL-23 (10

ng/mL) or Fla-C (5 μg/mL) for 24 h. Data are pooled from 3 independent experiments (n = 11 and 16).

(C) IL-22 production by untreated ileum explants from *Rorgt*^{Cre} *Ahr*$^{fl/fl}$ mice and their *Ahr*$^{fl/fl}$ littermates harvested on day 7 post-weaning and assayed 24 h after *in vitro* culture. Data are pooled from 4 independent experiments (n = 29 and 31).

(D) Serum FITC-dextran concentrations at 90 min post-gavage on day 7 post-weaning from *Rorgt*^{Cre} *Ahr*$^{fl/fl}$ mice and their *Ahr*$^{fl/fl}$ littermates. Data are pooled from 3 independent experiments (n = 26 and 25).

(E) Peanut sensitization timeline depicting weekly sensitization with peanut extract (PN) and cholera toxin by i.g. gavage for 5 weeks followed by challenge with PN by i.p. injection. Serum was collected after a booster injection at day 43. Some mice were euthanized at an earlier time point (day 17) to harvest splenocytes or lymph nodes for flow cytometric analysis or *in vitro* restimulation with antigen.

(F) IL-13 production after 72 h restimulation of splenocytes of PN-sensitized *Rorgt*^{Cre} *Ahr*$^{fl/fl}$ mice and their *Ahr*$^{fl/fl}$ littermates harvested on day 17 post-weaning. Data are pooled from 2 independent experiments (n = 22 and 17).

(G) PN-specific IgE and IgG1 in serum from PN-sensitized *Rorgt*^{Cre} *Ahr*$^{fl/fl}$ mice and their *Ahr*$^{fl/fl}$ littermates collected at euthanasia (day 43). Data are pooled from 2 independent experiments.

(H) Core body temperature change of mice in (G) at challenge (day 35) shown as mean temperature over time (left) and area under the curve values for each mouse (right). Data are pooled from 2 independent experiments (n = 12 and 10).

All bar graphs represent mean ± SEM and include individual data points; temperature data represents mean ± SEM. Significance was determined after log transformation using two-way ANOVA with Sidak's multiple comparisons test (A and B) or unpaired Student's t test.

See also Figure S5.

KEY RESOURCES TABLE

REAGENT or RESOURCE	SOURCE	IDENTIFIER
Antibodies		
Goat Anti-Mouse IgE-UNLB	SouthernBiotech	Cat#1110-01; RRID: AB_2794601
Goat Anti-Mouse IgG1, Human ads-HRP	SouthernBiotech	Cat#1070-05; RRID: AB_2650509
Rabbit anti-Goat IgG (H + L) Secondary Antibody, AP	Invitrogen	Cat#31300; RRID: AB_228392
CD3e Monoclonal Antibody, unconjugated, clone 145-2C11	Invitrogen	Cat#MA5-17655; RRID: AB_2539045
CD28 Monoclonal Antibody, unconjugated, clone 37.51	Invitrogen	Cat#14-0281-82; RRID: AB_467190
Monoclonal antibody against IL-22, clone 8E11	Genentech	RRID: AB_2651129
Isotype control antibody, clone GP120 10E7.1D2	Genentech	GP120 10E7.1D2
InVivoMAb anti-mouse CD16/CD32, clone 2.4G2	BioXCell	Cat#BE0307; RRID: AB_2736987
Hamster anti-mouse CD3e, APC/Fire 750, clone 145-2C11	BioLegend	Cat#100361; RRID: AB_2629686
Rat anti-mouse CD4, BV605, clone RM4-5	BioLegend	Cat#100548; RRID: AB_2563054
Rat anti-mouse Foxp3, FITC, clone FJK-16S	eBioscience	Cat#1-5773-82; RRID: AB_465243
Mouse anti-mouse RORgt, BV421, clone Q31-378	BD Biosciences	Cat#562894; RRID: AB_2687545
Anti-mouse Lineage Cocktail with Isotype Ctrl, PE	BioLegend	OldCat#78036 now Cat#133303; RRID: AB_1595553
Anti-mouse CD90.2, PE/Cyanine7, clone 30-H12	BioLegend	Cat#105326; RRID: AB_2201290
Rat IgG2b, k Isotype Control, PE-Cyanine7, clone eB149/10H5	eBioscience	Cat#25-4031-81; RRID: AB_891624
Armenian Hamster IgG, Isotype Ctrl, APC/Fire 750, clone HTK888	BioLegend	Cat#400962; RRID: AB_2923253
Rat IgG2a, k Isotype Ctrl, BV605, clone RTK2758	BioLegend	Cat#400540; RRID: AB_11126979
Mouse IgG2a, k Isotype Ctrl, BV421, clone MOPC-173	BioLegend	Cat#400260; RRID: AB_10960144
Rat IgG2a, k Isotype Ctrl, FITC, clone R35-95	BD Biosciences	Cat#553929; RRID: AB_395144
Bacterial and virus strains		
Bacteroides uniformis	Nagler lab	Stefka et al.[10]
Ruminococcus bromii	ATCC	ATCC 27255
Lach_1 (*Lachnospiraceae isolate*)	This study	N/A
Lach_2 (*Lachnospiraceae isolate*)	This study	N/A
LachOS_1 (*Lachnospiraceae + Oscillospiraceae* mix)	This study	N/A
LachOS_2 (*Lachnospiraceae + Oscillospiraceae* mix)	This study	N/A
Chemicals, peptides, and recombinant proteins		
Recombinant mouse IL-23	Invitrogen	Cat#14-8231-63
Flagellin (FLA-ST Ultrapure)	Invivogen	Cat#tlrl-epstfla-5
Indole	Sigma	Cat#I3408
Cholera Toxin (Azide-Free) from *Vibrio cholerae* Inaba 569B	List Biological Laboratories, INC	Cat#100B
Fluorescein isothiocyanate-dextran	Sigma	Cat#FD4
PureLink RNA Mini Kit	Invitrogen	Cat#12183025

REAGENT or RESOURCE	SOURCE	IDENTIFIER
iScript cDNA Synthesis Kit	BioRad	Cat#1708891
Quantinova SBR Green PCR Kit	Qiagen	Cat#208056
ELISA Max Deluxe Set Mouse IL-22 ELISA Kit	BioLegend	Cat#436304
Mouse IL-13 Uncoated ELISA kit	Invitrogen	Cat#88-7137-88
ELISA Max Deluxe Set Mouse IL-6 ELISA Kit	BioLegend	Cat# 431304
ELISA Max Deluxe Set Mouse CXCL1 ELISA Kit	BioLegend	Cat# 447504
LIVE/DEAD™ Fixable Aqua Dead Cell Stain Kit	Invitrogen	Cat#L34957
eBioscience™ Foxp3/Transcription Factor Staining Buffer Set	Invitrogen	Cat#00-5523-00
Deposited data		
-WGS contigs and trimmed reads for Lach_1, Lach_2, LachOS_1 and LachOS_2 -Shotgun metagenomic sequencing data for the whole cultured consortium (raw paired reads and full-consortium contigs file)	National Center for Biotechnology Information Sequence Read Archive	[SRA]: [SRR25527211] [SRA]: [SRR25527212] [SRA]: [SRR25528655] [SRA]: [SRR25528656] [SRA]: [SRR25528657]
Experimental models: Cell lines		
HEK-Blue™-mTLR5 cells	Invivogen	Cat#hkb-mtlr5
Experimental models: Organisms/strains		
Mouse: C57BL/6: C57BL/6J	Jackson Laboratory	JAX stock #000664
Mouse: *Ahr*$^{fl/fl}$: Ahr$^{tm3.1Bra}$/J	Jackson Laboratory	JAX stock #006203
Mouse: *Rorgt*^{Cre}	Yang-Xin Fu	Eberl et al.[51]
Mouse: *Myd88*$^{-/-}$: B6.129P2(SJL)-Myd88$^{tm1.1Defr}$/J	Jackson Laboratory	JAX stock #009088
Mouse: *Tlr5*$^{-/-}$: B6.129S1-Tlr5^{tm1Flv}/J	Jackson Laboratory	JAX stock #008377
Mouse: *Cd11c*^{Cre}: B6.Cg-Tg(Itgax-cre)1-1Reiz/J	Jackson Laboratory	JAX stock #008068
Mouse: *Myd88*$^{fl/fl}$: B6.129P2(SJL)-Myd88^{tm1Defr}/J	Jackson Laboratory	JAX stock #008888
Mouse: *Tlr5*$^{fl/fl}$: B6(Cg)-Tlr5$^{tm1.1Gewr}$/J	Jackson Laboratory	JAX stock# 028599
Mouse: *Tlr4*$^{-/-}$: B6(Cg)-*Tlr4*$^{tm1.2Karp}$/J	Nagler Lab	Matharu et al.[52]
Oligonucleotides		
See Table S1 for Primers used	See Table S1	N/A
Software and algorithms		
T-Coffee Multiple Sequence Alignment Program	Center for Genomic Regulation (CRG) Barcelona	https://tcoffee.org
PATRIC: Bacterial and Viral Bioinformatics Resource Center	The Bioinformatics Resource Centers	https://www.bv-brc.org/
BLAST: Basic Local Alignment Search Tool	NCBI	https://blast.ncbi.nlm.nih.gov/Blast.cgi

REAGENT or RESOURCE	SOURCE	IDENTIFIER
PHYRE2 Protein Fold Recognition Server	Structural Bioinformatics Group, Imperial College, London	http://www.sbg.bio.ic.ac.uk/~phyre2/html/page.cgi?id=index
SPAdes and metaSPAdes	St. Petersburg State University	https://cab.spbu.ru/software/spades/
RAST (Rapid Annotation using Subsystem Technology)	The Bioinformatics Resource Centers	https://rast.nmpdr.org/
prokka: Rapid prokaryotic genome annotation	The University of Melbourne	https://github.com/tseemann/prokka
ClustalOmega: Multiple Sequence Alignment	European Bioinformatics Institute	https://www.ebi.ac.uk/Tools/msa/clustalo/
IQ-TREE: Efficient phylogenomic software	IQ-Tree	http://www.iqtree.org/
Kraken 2 Metagenomic Analysis	Johns Hopkins University	https://ccb.jhu.edu/software/kraken2/
HMMR (hmmscan)	European Bioinformatics Institute	https://www.ebi.ac.uk/Tools/hmmer/search/hmmscan